

Comparing the Accuracy of Intra-Oral Scanners for Implant Level  
Impressions Using Different Scanable Abutments

THESIS

Presented in Partial Fulfillment of the Requirements for the Degree Master of Science in  
the Graduate School of the Ohio State University

By

Nakul H Rathi

Graduate Program in Dentistry

The Ohio State University

2014

Master's Examination Committee:

Dr. Edwin A. McGlumphy, DDS, MS (Advisor)

Dr. Burak Yilmaz, DDS, PhD

Dr. Robert Seghi, DDS, MS

Dr. Hua-Hong Chien, DDS, PhD

Copyright by

Nakul Rathi

2014

## **Abstract**

**Purpose:** This study was conducted to find the accuracy of digital intra-oral scanners (IOS) for fabricating computer aided designing (CAD)-computer aided manufacturing (CAM) implant supported prosthesis. The different IOS available have different technologies for data acquisition and processing. The IOS tested were 3M™ True Definition Scanner (3M ESPE, St.Paul, MN), iTero (Align Technologies, San-Jose, CA) and 3Shape Trios (3Shape Dental, Copenhagen, Denmark). The two scannable abutments tested were Encode® Healing Abutments (Bellatek, Biomet3i, West Palm Beach, FL)[ENC] and Zirkonzahn scan marker (Zirkonzahn.Modellier, Gais, Italy)[ZRZ]. The aim of the study is to check the accuracy of three IOS systems, for making virtual impressions for dental implants using two scannable abutments and two different implant angulations (Parallel and 30° angulation) to fabricate an implant supported bar.

**Materials and Methods:** A stereolithographic replica of a human mandible, with teeth #21 to #28 present, was fabricated. Posterior segments were edentulous. Four Full Osseotite® Certain implants (Biomet3i, West Palm Beach, FL) were placed in the posterior, 2 on each side; the implants on one side were parallel to each other and the implants on the other side diverged by 30°.

This model was digitized using a high-definition laboratory scanner (reference scanner, Sirona inEosX5, Salzburg, Austria) with two different scan bodies, ENC and ZRZ. 3Shape Design software was used to CAD the control and test bars.

IOS were made using three different intraoral scanners and similar bars were designed. A total of 36 test CAD bars were compared with 4 control bars. Digital files of the bars were loaded into 3D evaluation software (Geomagic DesignX™2013, Morrisville, USA). A virtual ‘one-screw test’ was done using “Global, Fine, Partial” alignment method in the software. For the alignment, centers of the abutment bases were not more than 5 $\mu$  away and the data points of alignment had more than 95% superimposition. After the ‘one screw alignment’ was achieved, gap height measurements (in  $\mu$ ) were made on the other side. The planar angle difference was measured and the final volume measurement was derived from the gap height and angular difference.

The calculated differences (mm<sup>3</sup>) were analyzed using a repeated-measures multifactorial ANOVA and Tukey-test, with an alpha level=0.05, with a non-directional alpha risk of 0.05. Post-hoc comparison was done showing all the possible combination of the variable types.

Four actual CAD bars were milled through the CAM process and compared to the digital analysis.

**Results:** The CAD-CAM prosthesis from the intra-oral scans had a misfit range of 12.40  $\mu$  to 90.20  $\mu$  all of which remained in the clinically acceptable range.

None of the three intra-oral scanners tested were more accurate than the others under all conditions. (p=0.0781).

Neither of the scannable abutments allowed more accurate implant impression than the other under all testing conditions. (p=0.5363)

Neither parallel nor angled implants allowed for more accurate impression than other under all testing conditions (p=0.3173).

Actual bars milled from these CAD files showed similar degree of misfit to the virtual data.

**Conclusions:** a. Geomagic Design X software analysis showed a similar virtual misfit to the actual physical misfit observed in fabricated milled bars, therefore the virtual one-screw test and design analysis of dental CAD-CAM prosthesis is a viable alternative for research in this area.

b. None of the three intra-oral scanners tested, 3M LAVA True Definition, 3Shape Trios and Cadent iTero were more accurate than the others under all conditions (p=0.0731).

c. Neither the Encode nor Zirkonzahn abutments allowed for a more accurate implant impression than the other under all testing conditions (p=0.5363).

d. The study suggests that digital intra-oral scanner impressions can be used for fabricating accurate short-span screw retained implant supported fixed dental prosthesis. (Misfit range of 12.40 to 90.20  $\mu$ )

## **Dedication**

Every challenging work needs self efforts as well as guidance of elders especially those who are very close to our heart.

My humble effort I dedicate to all those who have helped me get to where I am today. A special feeling of gratitude to my loving parents, Harish and Lata Rathi; there aren't enough words to describe their unending love and the support they have given in all of my endeavors.

My Grand-parents and the Rathi/Nagori Family, have always empowered me with their blessings, encouragement and lessons of wisdom. My sister, Neha Sarma has been the pillar of my strength, my emotional and moral support, my best cheerleader throughout this wonderful journey.

I would like to accord a special thank you to my nephews Siddharth and Samarth for being a part of my life.

Thank You All

## **Acknowledgments**

I wish to express my gratitude to my committee members Dr Edwin McGlumphy, Dr. Burak Yilmaz, Dr. Robert Seghi and Dr. Hua-Hong Chien who were more than generous with their guidance, expertise and precious time. A special thanks to Dr. Edwin McGlumphy, my thesis advisor for his countless hours of reflecting, reading, encouraging, and most of all patience throughout the entire process. This project would not have been possible without your thought provoking ideas, inspiration, push for tenacity and clinical wisdom. Your unbridled passion for advancement in dentistry helped me realize my potential and, make this contribution to modern digital dentistry. I am indebted to Dr. Kent Howell for the Models that I used for the study. Dr. Frank Beck and Dr. Johnston, I appreciate your willingness to take the time from your schedule to teach me the statistics and mentor me through the statistics. Jason Kientz, from fixed lab at OSU, Brandon Smidth from Henry Schein and Dr. Neal Patel from Infinite dental smiles, I appreciate your consistent kindness for helping me in the acquisition of scan data. A special thanks to ROE Dental Lab for the milling designs and fabrication of the CAD Bars. Gregory Knapik from the Biodynamic Research Lab for for being a gracious sound-board for brainstorming and for helping me with the Geomagic Desgin X and Geomagic Verify software permissions and basic training.

Finally I would like to thank my co-residents. Their excitement and willingness to provide feedback made the completion of this research an enjoyable experience.

## **Vita**

Date and place of birth: June 4<sup>th</sup>, 1986  
Nagpur, Maharashtra, India

09/2004 -10/2009 Bachelor of Dental Surgery (B.D.S.),  
Government Dental College & Hospital,  
Nagpur, Maharashtra, India.

06/2004 -04/2007 Bachelor of Business Administration (B.B.A.),  
ICFAI, (Distance Learning)  
Dehradun, India.

10/2009 -06/2010 Implant Dentistry Course: Implant Continuum,  
New York University, College of Dentistry,  
New York, New York, USA

06/2011-Present Advanced Prosthodontics (M.S.)  
The Ohio State University, College of Dentistry,  
Columbus, Ohio, USA

## **Publications**

- Rathi, N., Scherer, M. D. and McGlumphy, E. Stabilization of a Computer-Aided Implant Surgical Guide Using Existing Dental Implants with Conversion of an Overdenture to a Fixed Prosthesis. *Journal of Prosthodontics*. Jun 2014.  
doi: 10.1111/jopr.12174.
- Scherer ,MD, Ingel ,AP, Rathi ,NH. “Flap or Flapless narrow diameter implant surgery for overdentures: advantages, disadvantages, indications, and clinical rationale.”. *International Journal of Periodontics and Restorative Dentistry*. 2014;34(suppl):s89–s95.
- Rathi, NH, Heshmati, RH, Yilmaz, B, Wilson, WH. “A technique for fabricating a hinged mandibular complete dental prosthesis with Swing-lock for a patient with microstomia”. *Journal of Prosthetic Dentistry*. Dec 2013; 110(6):540-3

## **Fields of Study**

Major Field: Dentistry

## Table of Contents

Abstract .....	ii
Dedication .....	v
Acknowledgments.....	vi
Vita.....	vii
Publications.....	viii
Fields of Study .....	viii
Table of Contents .....	ix
List of Tables .....	xi
List of Figures .....	xii
Chapter 1 : Introduction .....	1
1.1    New Implant Impression Techniques.....	5
1.2    Intra-Oral Scanning Impression .....	10
1.3    Specific Aims and Hypothesis: .....	14
Chapter 2: Material and Method.....	15
2.1    Master Model and Control Bar Designing .....	15
2.2    Test Scanning .....	28

2.3	Data Collection Process: .....	32
2.4	Data Evaluation and Statistical Analysis .....	39
2.5	Comparison of Virtual Test with CAM-Titanium Bars .....	39
Chapter 3: Results .....		41
3.1	Abbreviations Used .....	41
3.2	Volume Misfit Results .....	46
3.3	Gap-Height Distance Misfit Results: .....	47
3.4	Angle Misfit Results : .....	48
3.5	ANOVA Summary:.....	49
3.6	Results of the Post-hoc analysis.....	54
3.7	Results of Sheffield Test (One Screw Test) of the Milled bars .....	55
Chapter 4: Discussion .....		58
Chapter 5: Conclusion.....		64
Bibliography .....		66

## **List of Tables**

Table 1: List of Intra-oral scanning systems.....	11
Table 2 : Test Scanners .....	14
Table 3: Control Laboratory Scanner .....	14
Table 4: Gap-Height Distance and Angle Deviation Data.....	42
Table 5: Volume Deviation Data .....	43
Table 6: Summary data .....	44
Table 7: ANOVA summary .....	49
Table 8: Post hoc comparisons .....	51
Table 9: Howell et al data of the same model with conventional impression techniques <sup>xvi</sup> .....	61

## List of Figures

Figure 1: Closed tray technique or the transfer type technique. ....	2
Figure 2: Open tray technique, or the pick-up technique .....	3
Figure 3: Encode® Healing Abutment from Bellatek, Biomet 3i. ....	5
Figure 4: Encode® Abutment intraoral view.....	6
Figure 5: Robocast™ Milling Machine. ....	6
Figure 6: Robot preparing analog space and emergence .....	8
Figure 7: Cyanoacrylate added to space created by robot for fixation of implant analog to robocast completed robocast with analogue. <sup>xvii</sup> .....	9
Figure 8: Confocal Microscopy and Itero Wand ,, .....	12
Figure 9: Active wavefront sampling used in 3M True Definition <sup>xxiv</sup> .....	12
Figure 10: Master model showing the implants placed .....	17
Figure 11: Master model with Zirkonkahn abutments.....	17
Figure 12: Model showing the angled implants side with the Zirkonzahn abutments. ....	18
Figure 13: Encode healing abutment (ENC).....	18
Figure 14: Zirkonzahn ScanAbutment (ZRZ).....	19
Figure 15: Master model with Encode Healing Abutments (ENC).....	19
Figure 16: Model showing the angled implants side with ENC .....	20
Figure 17 :Control Lab Scanner Sirona inEos. X5 .....	20
Figure 18: Control Scan A: With Encode Abutment (ENC) .....	21

Figure 19: Control Scan B: With Zirkozahn Abutment (ZRZ).....	21
Figure 20: Scan opened in the 3Shape Design software and Orientation of the casts done. .....	22
Figure 21: Library CAD-file of the abutment used for alignment.....	22
Figure 22: Three-point alignment technique used for CAD-file alignment. ....	23
Figure 23: Three-point alignment completed. ....	23
Figure 24: Virtual implant analogues placed to make a CAD cast.....	24
Figure 25: Designing of the bar .....	24
Figure 26: Designing of the bar .....	25
Figure 27: Designing of the bar .....	25
Figure 28: Designing of the bar .....	26
Figure 29: Milling of the bars. ....	26
Figure 30: CAD-CAM bars. ....	27
Figure 31: CAD-CAM on the cast.....	27
Figure 32: Fit checked with one-screw test.( Sheffield Test .....	28
Figure 33: (Top right) 3Shape Trios, (Top Left) Cadent iTero, (Bottom)3M Lava True Definition .....	29
Figure 34: Occusal view of scan made from 3Shape Trios Scanner .....	30
Figure 35: Facial view of scan made from 3Shape Trios Scanner .....	30
Figure 36: Computer Aided Design of the bars made on parallel (pink) and divergent(yellow) implants. ....	31

Figure 37: Virtual one-screw test using the Geomagic Desin X. “GLOBAL and FINE and PARTIAL” alignment method. (Light Blue points show the area that is superimposed.)	33
Figure 38: Histogram showing the level of alignment. More than 95% and Less than 5microm gap height on the aligned side. ....	33
Figure 39: Screenshot of the Geomagic Design X software used for making the virtual measurements.....	35
Figure 40: The misfit shown at the control ( Blue) vs the test (Red) abutment.....	35
Figure 41: CAD view of the abutment showing the abutment-implant interface where measurements were made. (Blue colored abutment is the Control Abutment and the Green Colored abutment is the Test Abutment) .....	36
Figure 42: Enlarged view of the center of the abutments showing gap-height measurements being made. ....	36
Figure 43: Gap height (distance measurement done between the control and the test )...	37
Figure 44: Enlarged view of the abutment showing the abutment implant interface where the angle deviation measurements were made.....	37
Figure 45: Planar angular difference measurement done between the control and the test .....	38
Figure 46: Diagramatic representation of the Volume misfit. ....	38
Figure 47: Geometrical formula used for calculating the approximate value of the volume misfit. ....	39
Figure 48: Titanium CAD-CAM Bars used for doing Sheffield Test (One-Screw Test).	40
Figure 49: Volume Misfit Results.....	46

Figure 50: Gap-Height Distance Misfit Results.....	47
Figure 51: Angle Misfit Results.....	48
Figure 52: ANOVA Summary .....	50
Figure 53. Actual CAD-CAM Bar one-screw test with good fit. ....	55
Figure 54: Close-up view of the precisely fitting bar made from the Control Scanner....	56
Figure 55: Actual CAD-CAM Bar one-screw test showing the gap .....	56
Figure 56: Close-up view of the Gap height difference noted in the bar made from the least accurate designed bar as per the CAD assessment. ....	57
Figure 57: Clinical Situation showing a one screw test.....	59
Figure 58: Virtual One-Screw Test Done on Geomagic Design X .....	59
Figure 59: Actual CAD-CAM Bar one-screw test showing the gap .....	60

## Chapter 1 : Introduction

Dental implants have become a very successful restorative treatment modality in contemporary clinical dentistry. Over the past thirty years, since Prof. P. I. Branemark first introduced Osseointegration, dental implants have become an integral part of a dentist's armamentarium of treatment options for a lot of patients.<sup>i</sup> But despite the high success rate and the predictability of the treatment<sup>ii,iii,iv,v</sup> the modality has not been adopted by all dentists. Complexities involved with this process may be the reason why more than a third of general dentists, do not routinely offer implant restoration services at their practices.<sup>i</sup> One survey suggest that only about 61% of dentist offer implants as an option to their patients.<sup>vi</sup>

There are complexities both at the surgical stage and the restorative phase. Technological advances with Computer Tomography, Guided surgeries and good diagnostic tools are making the surgical aspect more predictable and less complex.<sup>vii</sup> One of the reasons for the unfamiliarity and lack of use of implants in dentistry is the perceived difficulty in making implant impressions. Any advancement in implant restoration protocols that can simplify the restorative dentist's role in this process has the potential to increase the number of dentists who offer implant restoration services. With more dentists offering implant therapy, better dental care can be provided to the population in general.

For the fabrication of implant supported crowns or fixed partial dentures, the first step is making an accurate implant level impression. The foundation of a good fitting prosthesis is established at the impression stage. Impressions are the reproduction of patients' intra-

oral hard and soft tissue contours. When this negative reproduction is poured using dental gypsum an actual replica of the patients' mouth is obtained. Traditionally, for obtaining implant position and three dimensional orientation of the dental implants, two techniques have been described. The "open tray" technique (or pick-up technique) and the closed tray technique (the transfer type) have both been utilized for the longest amount of time in implant prosthodontics.



Figure 1: Closed tray technique or the transfer type technique.<sup>viii</sup>

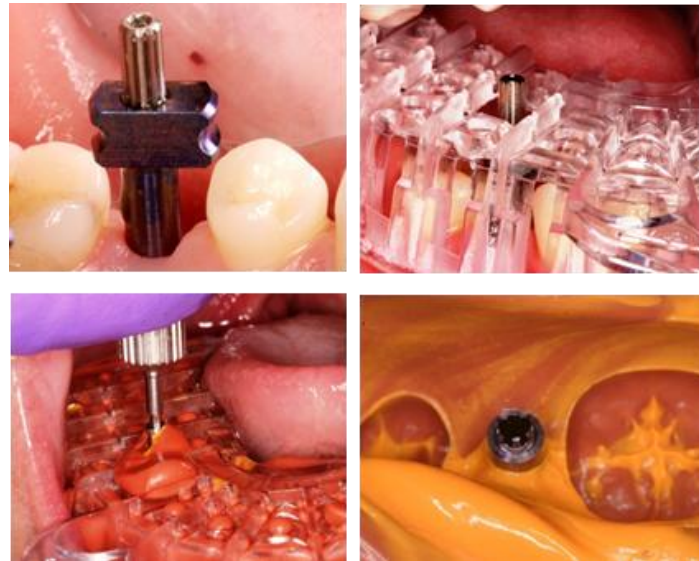


Figure 2: Open tray technique, or the pick-up technique<sup>viii</sup>

Traditionally the clinician and the laboratory technician made elastomeric impressions and gypsum casts. Impression techniques for implant treatment were modifications of conventional prosthodontic techniques. Because the shape of the pre-machined implant or abutment is known, attention can be focused on the relationship between the implant and the surrounding teeth, rather than on the reproduction of its shape. Reports on materials and techniques used to fabricate casts in implant dentistry have not been consistent with regard to which technique is most accurate<sup>ix x xi xvii</sup>. Both early and recent studies on implant impression procedures report that working casts fail to exactly replicate the original situation and that no single impression procedure is more reliable than others under all circumstances.<sup>xviii xii</sup> The accuracy of these master casts for making the restoration has been subject to numerous research projects. Some of the reasons for accuracy variation of master cast include water/powder ratio, vacuum/hand mixing<sup>ix</sup>, type of the dental stone and its compatibility with the impression materials<sup>ix xiii</sup>,

impression materials, impression tray types, impression techniques, implant position transfer technique etc.<sup>xiv</sup> The inaccuracies in the cast may be because of displacement of the implant components that can be introduced in three main ways, namely:

- (i) displacement of each impression coping on the fitting surface of each implant across the machining tolerance range;
- (ii) displacement of each impression coping, the degree of displacement depending on the impression technique or the material used;
- (iii) displacement of implant analoges on the fitting surface of each impression coping in the impression across the machining tolerance range <sup>xviii</sup>.

The angulation of the implants also has a significant effect on the accuracy of the impression and casts made. Assuncao et al. showed that open tray impressions are more accurate than closed tray when the implants are more divergent.<sup>xv</sup> Each step introduces potential human and/or material error<sup>ix xvii xii</sup>. The initiation factor which can have the maximum impact on the accurate and superior fit of the restoration is the foundation laid by an accurate impression. The current state of material properties involving the shrinkage of the impression material and the expansion of the gypsum along with possible splinting of the impression posts whenever needed, make fairly accurate casts which are clinically acceptable. But, the complexity level, technique and the technique sensitivity still remains the same as it was at least 30 years ago. The digitization of this technique has the potential to counter a lot of these errors. So, in this project, Computer Aided Designing and Computer Aided Manufacturing (CAD-CAM) was evaluated to determine if it was beneficial to the process.

## 1.1 New Implant Impression Techniques

To meet this prosthetic demand of making implant impressions simpler for dentists, Biomet 3i Corporation developed a novel implant restoration technique that allows the restorative doctor to complete an implant case with just one impression, without using any additional hardware components. The “Encode” system is an available option for surgical dentists who wish to promote implant restorative dentistry to those among their referral base who are not familiar or comfortable with implant dentistry. This method allows for the fabrication of suitably contoured implant abutments, without the need for restorative dentists to make implant level impressions. The Encode Impression System consists of two-piece healing abutments and the resultant titanium and zirconium patient specific abutments. Encode® Healing Abutments (ENC) (Fig 3,4) contain specific markings on the coronal surfaces that can be used by a computer software program to identify the implant platform diameter, hex position (in three dimensions), and healing abutment height.



Figure 3: Encode® Healing Abutment from Bellatek, Biomet 3i.



Figure 4: Encode® Abutment intraoral view.



Figure 5: Robocast™ Milling Machine.

The healing abutment can be placed on the implants by the surgeon at the second stage surgery or the implant uncovering step and then the soft tissue is allowed to heal around this ENC. After the peri-implant soft tissues has healed to conform to the size and shape of the healing abutment, an elastomeric impression of the Encode healing abutment can be made and poured with low-expansion dental stone per manufacturer's recommendation. The master cast, opposing cast and inter occlusal registration are scanned and the data is digitized. The scan is then uploaded into 3Shape CAD software, where the information is processed and related to one another. The CAD technician identifies the Encode® codes on the healing abutments, and the codes are overlaid with a "perfect" healing abutment on file. This process is done to analyze the accuracy of the scan of the occlusal codes. Once verified, a virtual implant analog is placed within the software to depict the implant within the patient's mouth.<sup>xvi</sup> The digitized data is sent to another part of the facility to prepare the master cast for analog placement with Robocast™ technology. (Fig 5,6) The cast is evaluated and it is placed on the robot's magnetic mount in the same manner as it was in the 3Shape scanner. As part of the abutment design, optimal emergence for the restoration is the first part of the Robocast™ to be completed.<sup>xvi</sup> The emergence profile is done by using a larger bur to make the general outline of the emergence in the stone cast. Before the outline form is created, the robot selects the correct sized bur and scans the edges of the bur with a laser to calibrate the robot. Once calibrated, the robot creates the emergence outline by carving it into the stone cast; this bur is then replaced with a smaller bur that is appropriate for the diameter of the planned implant analog to be placed. This bur is also calibrated with the laser, the

cast is oriented on the table and the analog hole is drilled. The robot drills perpendicular to the horizontal plane; it is the magnetic base that moves the cast for drilling. The technician then selects the correct implant analog for the case and places it into the robot. Cyanoacrylate is applied to the inside of the stone hole by the technician; the robot puts the analog into place and maintains its position.(Fig 7) <sup>xvi</sup>



Figure 6: Robot preparing analog space and emergence <sup>xvi</sup>

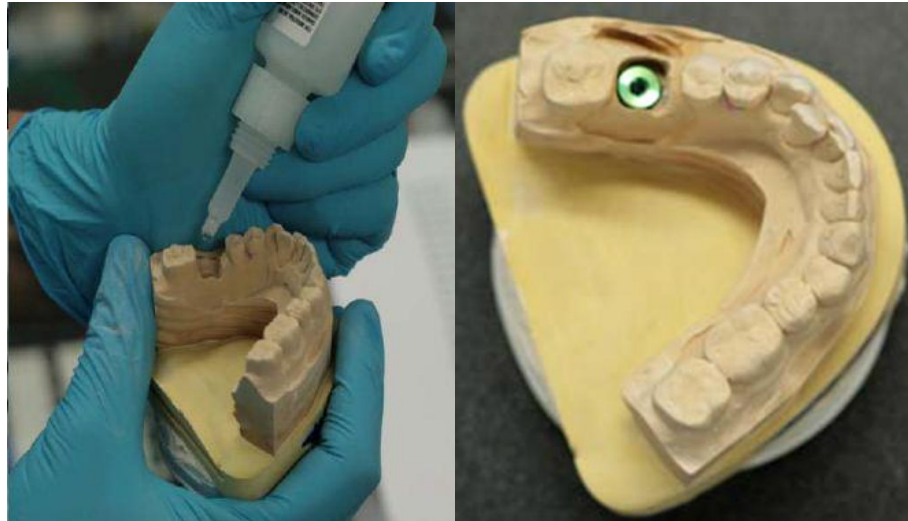


Figure 7: Cyanoacrylate added to space created by robot for fixation of implant analog to robocast completed robocast with analogue. <sup>xvii</sup>

The results from Howell et al. study<sup>xvii</sup> at The Ohio State University and also from a similar study from Sweden by Eliasson et al.<sup>xviii</sup> showed that the newer technique, although easier, was significantly less accurate than the conventional open and closed tray impressions. An in-vitro comparison of the accuracy of the robocast by Al-Abdulla et al<sup>xix</sup> concluded that the implant definitive casts fabricated from the coded healing abutment impressions were found to be less accurate than those fabricated from the open tray impressions. This study was done with a splinted impression coping technique for restoring 2 paired (10° or 30°) convergent internal connection implants with nonengaging screw-retained splinted 2-unit implant restorations.<sup>xix</sup> Accuracy of fit was not influenced by the implant angulation or position for either impression technique or by the ENC height for the Encode impression technique.<sup>xix</sup> The possible reason for that have been discussed in their studies as impression material inaccuracies and stone, Robocast™

tolerance, the adhesive that is used for luting the analogue to the cast etc.<sup>xvi xvii</sup> Therefore this technique actually has the disadvantages of the older techniques and the new potential sources of errors. Digitization of the data earlier would possibly be the solution which directs the discussion towards intra-oral scanning.

## **1.2 Intra-Oral Scanning Impression**

Clinicians all over the world desire to eliminate the physical dental impression from their armamentarium. At almost the same time when implants were going global, the University of Zurich Dental School in September 1985 fabricated the first CEREC® restoration<sup>xx</sup>. Computer Aided Design/Computer Aided Machining (CAD/CAM) was first introduced into dentistry by Duret in 1988<sup>xxi</sup>. Duret designed the first chair side intra oral scanning device that used computer aided design (CAD) to scan prepared teeth, and then, with a computer software program, designed and milled functional replacement ceramic restorations.

Around the same time, others were working on similar systems and ideas with CAD/CAM technology. In 1989, Mörmann published his first article as the developer of the CEREC® system<sup>xx, xxii</sup>. CEREC® has continued to develop their product and many consider them to be one of the most successful CAD/CAM dental systems in the world. There are many more companies that have come up with similar intra-oral scanning systems.<sup>xxiii</sup> Examples :

Table 1: List of Intra-oral scanning systems

S.No.	Scanner Name	Company
(1)	CEREC	Sirona Dental System GmbH(Germany)
(2)	iTero	CADENT Ltd(Israel)
(3)	E4D	D4D TECHNOLOGIES, Llc(USA)
(4)	Lava <sup>TM</sup> True Definition	3M ESPE (USA)
(5)	IOFastScan	IOS TECHNOLOGIES, Inc.(USA)
(6)	MIA3d <sup>TM</sup>	Densys3D Ltd(Israel)
(7)	DPI-3D	DIMENSIONAL PHOTONICS INTERNATIONAL, Inc. (USA)
(8)	3DProgress	MHTS.p.A.(Italy )and MHT Optic Research AG(Switzerland)
(9)	DirectScan	HINT – _ELSGmbH(Germany)
(10)	Trios	3SHAPES A/S(Denmark)
(11)	Bluescans-I	A_TRON3Ds GmbH (Austria)
(12)	Planscan	Planmeca Oy(Finland)
(13)	Condor	Remedent Inc.(Belgium)
(14)	CS3500	Carestream Health,Inc.(USA)
(15)	DigImprint	Steinbichler Optotechnik GmbH(Germany)

Most of the systems use different types of technology to scan, mainly:

1. Confocal Laser Scanner Microscopy - Itero and 3 Shape have that
2. Triangulation techniques - Cerec , IOS Fast Scan
3. Optical Coherent Tomography - E4D
4. Active Wavefront sampling-3M Lava



Figure 8: Confocal Microscopy and Itero Wand ,<sup>xxiii</sup> <sup>xxiv</sup>

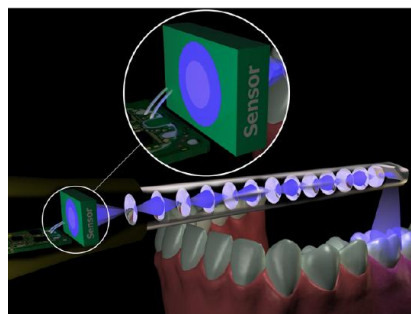


Figure 9: Active wavefront sampling used in 3M True Definition<sup>xxiv</sup>

Moreover, now with the use of Intra-Oral Scanners (IOS), the steps of making impressions of the encode abutment can also be changed and done through the scans of the abutments directly in the mouth. This will potentially make the clinical steps even easier and dentist friendly.<sup>xxv</sup> In recent times, newer systems have developed, which use scan abutments of different shapes and sizes. Example include: ones from Zirkon-Zahn, Inclusive from Glidewell Dental Lab and Flo-Kit Abutments from Dentsply etc. These new scanable abutments are often being used for capturing the position of implants after the physical gypsum casts have been made. However, the direction of advances in IOS and the accuracy shown by them for regular restorative work is encouraging.<sup>xxvi</sup> There have been anecdotal case reports showing the successful use of these abutments with

IOS. Nayyar et al showed predictable single unit crowns that were made<sup>xxvii</sup> and Wei-Shaao Lin 2014<sup>xxviii</sup> made a full arch fixed implant supported prosthesis. But there have not been many publications to show the accuracy of IOS for implant impressions.

Also, the fit of implant supported fixed partial dentures made using IOS has not been documented. Passive fit of implant prosthesis is important, but the level of acceptable misfit has been debated a lot in the scientific literature. In 1983, Brånemark was the first to define *passive fit* and he proposed that it should exist at the 10 micron to enable bone maturation and remodeling in response to occlusal loads.<sup>i</sup> In 1991, Jemt<sup>xxix</sup> defined a level of passive fit that did not cause any long-term clinical complications. It was suggested that misfits smaller than 150 micron were clinically acceptable<sup>xxix</sup>. It was proposed that an unacceptable level of framework misfit existed when greater than half-a-turn was needed to completely tighten the gold screw after its initial seating resistance was encountered<sup>xxix</sup>. Although the preceding values were reported and subsequently highly quoted, they are of empirical origin.<sup>xxx</sup> There are various methods of evaluation of the framework fit like alternate finger pressure technique, direct vision and tactile sensation, radiographs etc.<sup>xxx</sup> One of the most commonly used ones is the “One-Screw Test” described by White in 1991. It is also called the Sheffield test.<sup>xxxi</sup>

This commonly used determinant to check the implant-supported FPD’s misfit is the gap-height distance,<sup>xxxii</sup> but, in theory, the misfit is actually in Volumetric error.<sup>xxxiii</sup>

Therefore the study was designed to calculate this volume misfit between the prosthesis made with different IOS.

Table 2 : Test Scanners

Sr. No.	Scanner Type	Company / Model
1.	Impression using a Chair-side oral scanner	3M / True Definition
2.	Impression using a Chair-side oral scanner	Cadent/ iTero
3.	Impression using a Chair-side oral scanner	3Shape/ Trios

Table 3: Control Laboratory Scanner

Sr. No.	Type of Scanner	Company / Model
1.	Scan of the model with a Lab Scanner	Sirona/ InEOS X5

### 1.3 Specific Aims and Hypothesis:

There are few studies that evaluate the accuracy of CAD-CAM prosthesis<sup>xxxiv</sup>, which are made using IOS data. The aim of the study was to check the accuracy of Intra-Oral Scanner(test scanners) for making impressions for dental implants, using two scannable abutments and two different implant angulations. The accuracy of short span implant supported bar was checked by comparing the bars designed from the test scanners with the one fabricated using the laboratory scanner.

There were three hypotheses to be tested:

The first null hypothesis was that there was no difference in accuracy of impressions made with the three intra-oral scanners for making implant prosthesis.

The second null hypothesis was that, the use of different shape of the scan abutment did not affect the accuracy of the implant prosthesis that was made using intra-oral scans.

The third null hypothesis was that, the relative angularity of the implant fixtures did not affect the accuracy of these intra-oral scan impressions.

## **Chapter 2: Material and Method**

### **2.1 Master Model and Control Bar Designing**

To simulate any edentulous site with implants, a stereolithographic model replica of human mandible was used as 'patient' for this study. This mandible had bilateral posterior edentulism and 4 Biomet 3i implants were placed in #18, 20, 29 and 31. (fig.10) #29 and #31 were placed parallel (P) and #18 and #21 were placed with 30° divergence.(D) (fig.11 to 15)

To check what design of scan body was more accurate in getting information for intra-oral scans, two designs of scan bodies were used. [Bellatek Encode fig.13 and Zirkon-Zahn fig.14]. This model was first scanned in a high-definition laboratory scanner (Sirona InEoS X5) (Fig. 17) by screwing Zirkon-Zahn scan abutments (ZRZ) onto all four implants and then replaced by four abutments Encode Abutments (ENC) (Fig. 11, 12, 15, 16). After the ZRZ were placed, one more high-definition scan was obtained from the laboratory scanner. These two initial scans acted as the control scans for the study. (Fig. 18,19)

The reference scans were used to do the computer aided designing of two non-engaging screw retained bars on a dental prosthesis design software. (3Shape Design). The bar on the divergent implants #18 and #20 was designed on the left of the master scan model and

the bar on the parallel implants #29 and #31 was designed on the right side of the master scan model. (Fig. 20-28)

The CAD bars designed from the control scanner acted as the 'Control Bars'.



Figure 10: Master model showing the implants placed

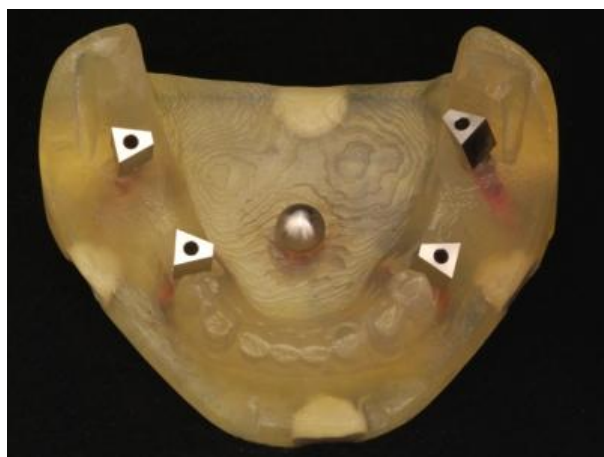


Figure 11: Master model with Zirkonkahn abutments.



Figure 12: Model showing the angled implants side with the Zirkonzahn abutments.



Figure 13: Encode healing abutment (ENC)



Figure 14: Zirkonzahn ScanAbutment (ZRZ)



Figure 15: Master model with Encode Healing Abutments (ENC)



Figure 16: Model showing the angled implants side with ENC



Figure 17 :Control Lab Scanner Sirona inEos. X5



Figure 18: Control Scan A: With Encode Abutment (ENC)

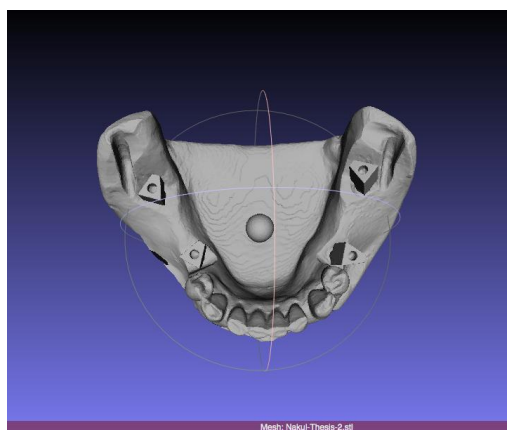


Figure 19: Control Scan B: With Zirkonzahn Abutment (ZRZ)

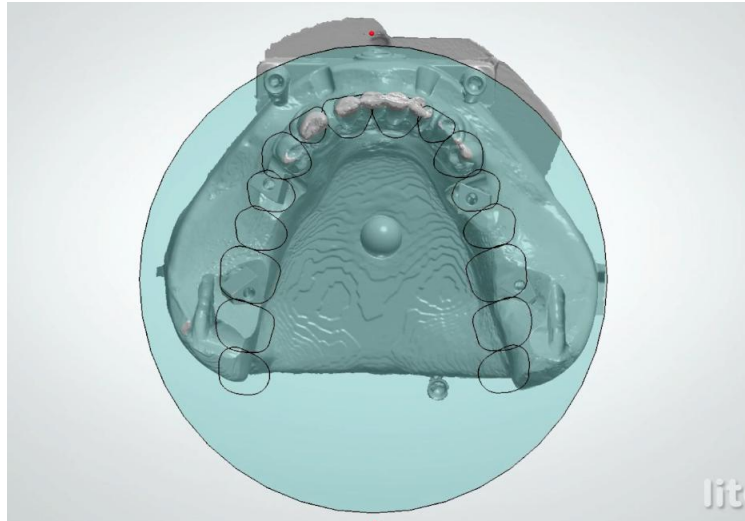


Figure 20: Scan opened in the 3Shape Design software and Orientation of the casts done.

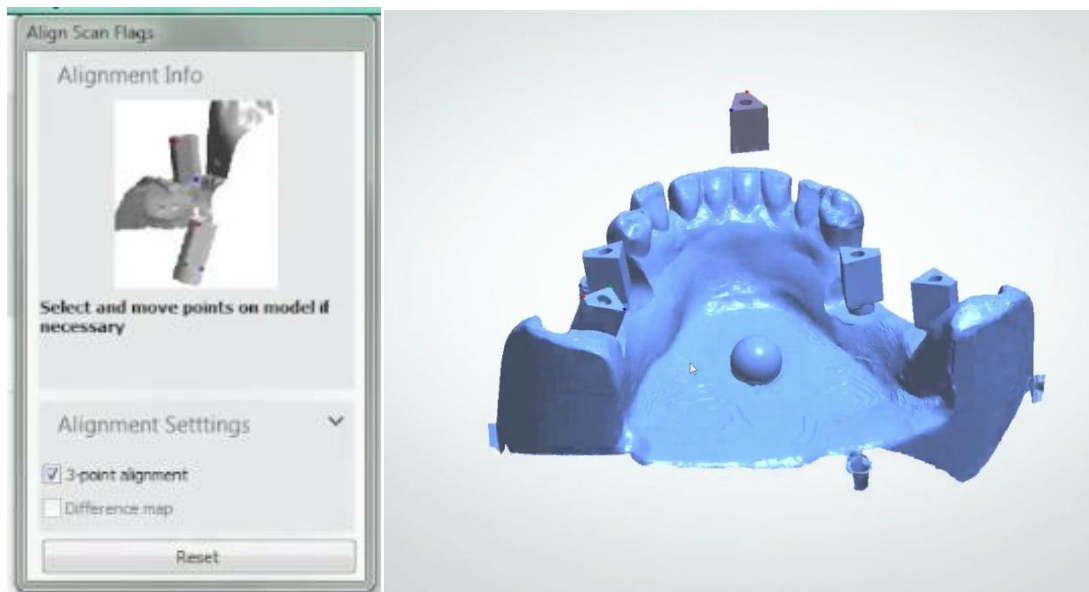


Figure 21: Library CAD-file of the abutment used for alignment.

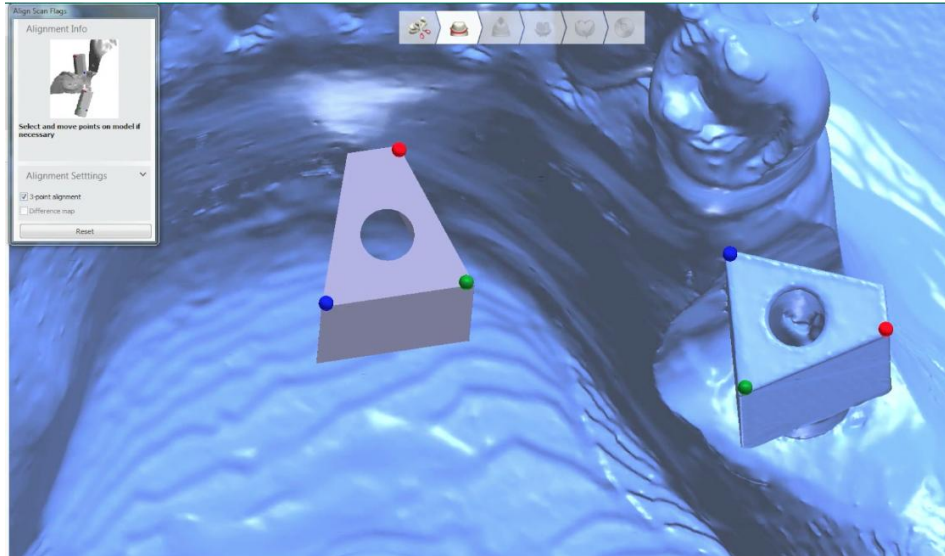


Figure 22: Three-point alignment technique used for CAD-file alignment.

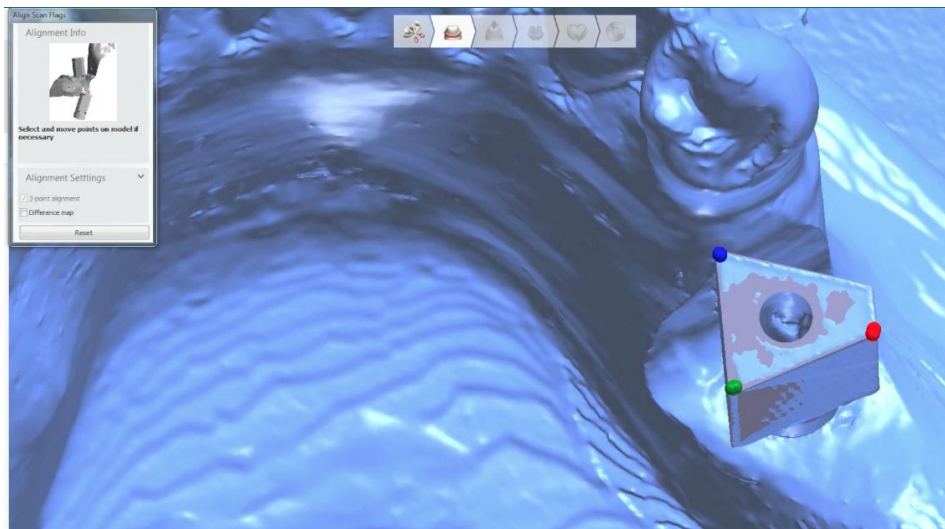


Figure 23: Three-point alignment completed.

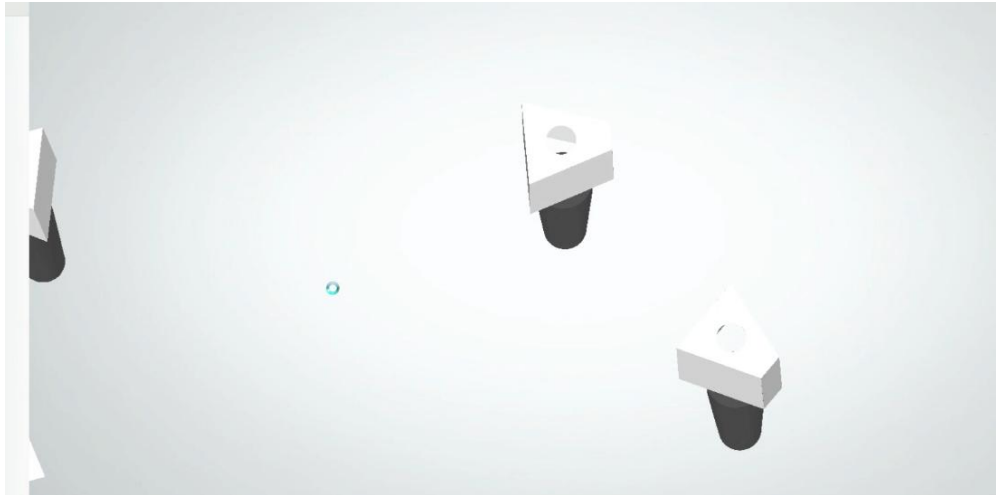


Figure 24: Virtual implant analogues placed to make a CAD cast.

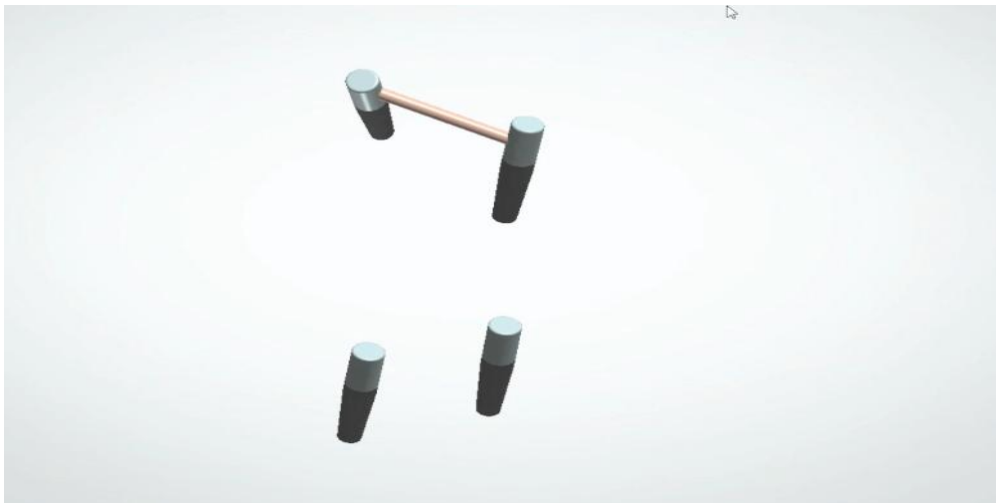


Figure 25: Designing of the bar

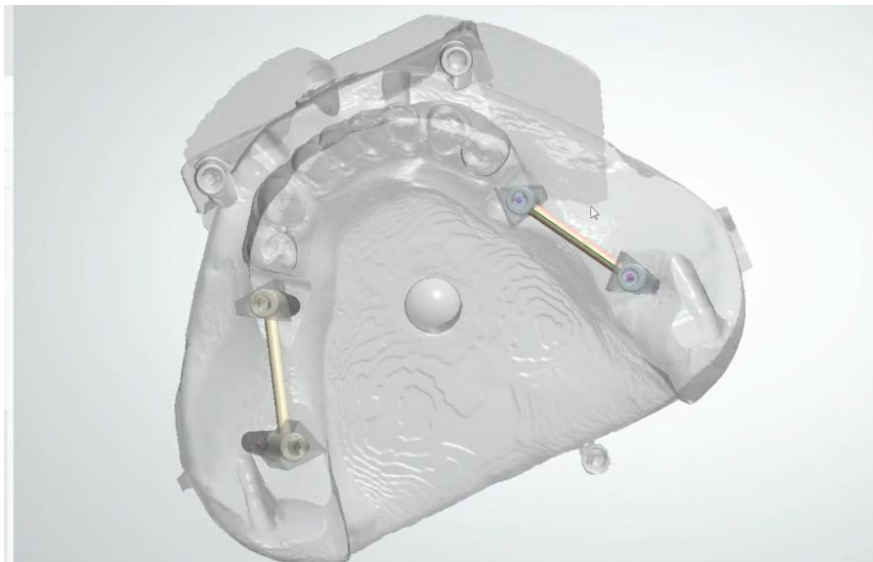


Figure 26: Designing of the bar



Figure 27: Designing of the bar



Figure 28: Designing of the bar



Figure 29: Milling of the bars.<sup>xxxv</sup>



Figure 30: CAD-CAM bars.

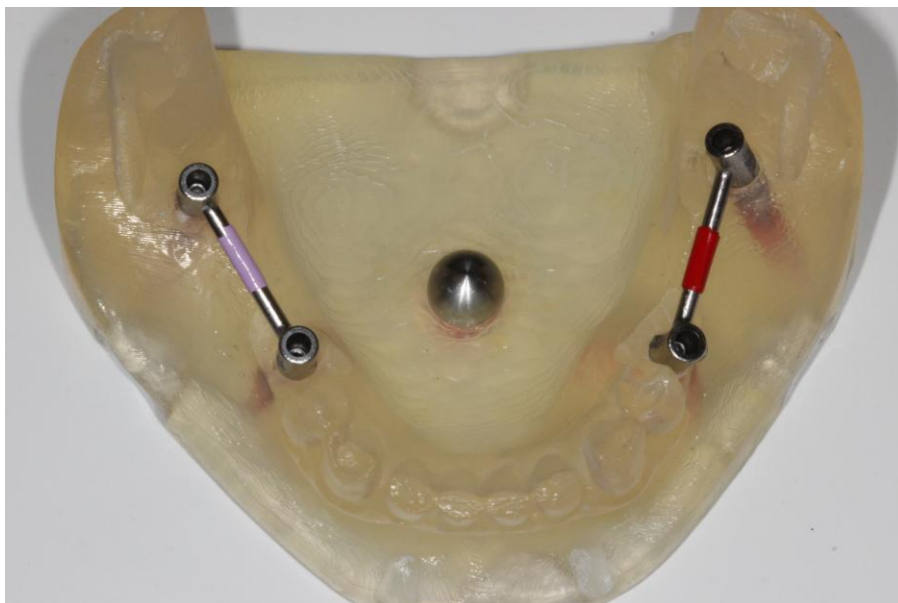


Figure 31: CAD-CAM on the cast.

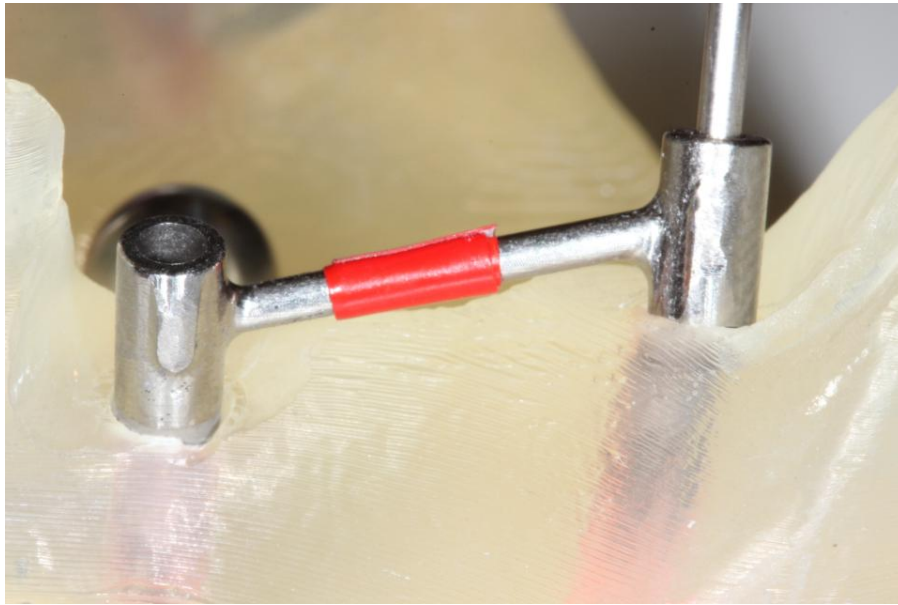


Figure 32: Fit checked with one-screw test. (Sheffield Test)

## 2.2 Test Scanning

The model was scanned with the three test scanners to be tested. The master cast had two parallel implants and two divergent implants. Three different intra-oral scanners, 3M TrueDefinition, Cadent iTero and 3Shape- Trios, (Fig. 33) were used to make the impression of implants on the master model with two types of scanable abutments ENC and ZRZ. (Fig. 13,14)

A total of six scans were made from each test scanner, three with all Encode abutments and three with the Zirkon-Zahn Abutments. A total of 18 scans were obtained. (Fig. 34,35)



Figure 33: (Top right) 3Shape Trios, (Top Left) Cadent iTero, (Bottom)3M Lava True Definition

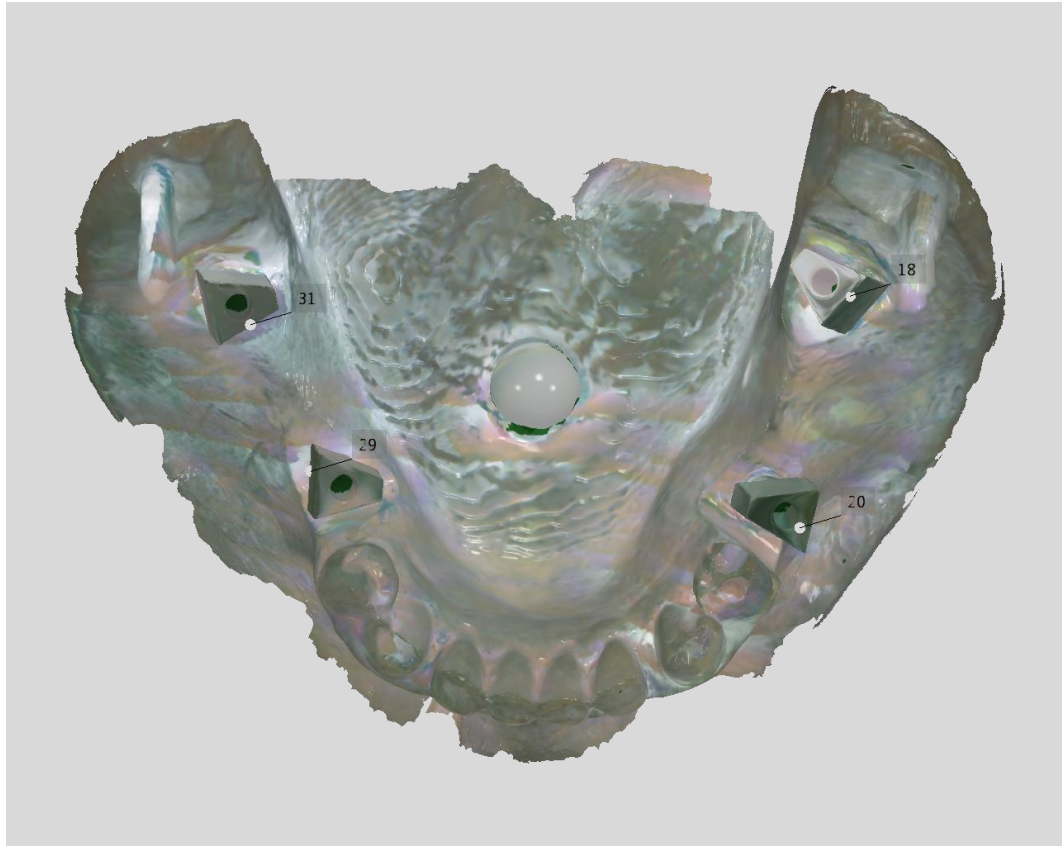


Figure 34: Occlusal view of scan made from 3Shape Trios Scanner

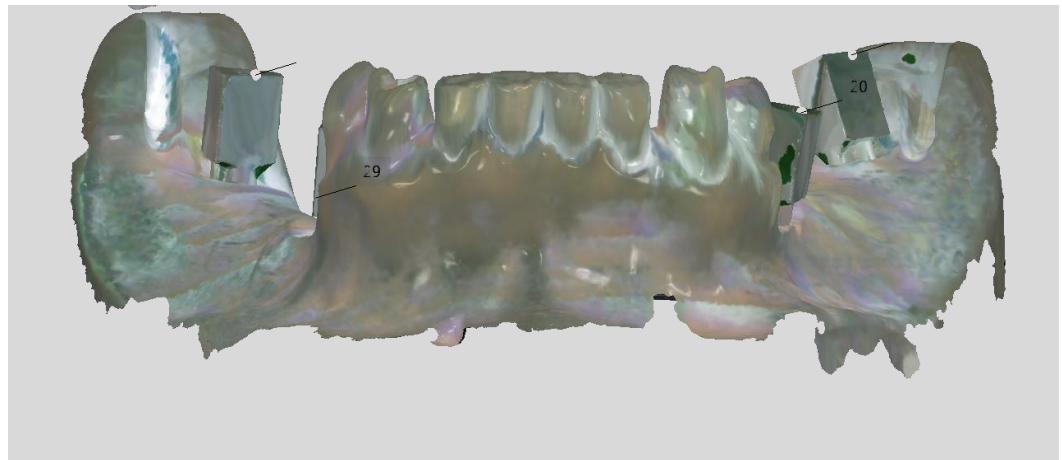


Figure 35: Facial view of scan made from 3Shape Trios Scanner

The scan from this procedure was processed and same cylindrical abutments were placed virtually on the CAD file. (Fig. 36)

Computerized measurements were made of the accuracy of the analog transfers in the master casts to the locations of the master model implants and these measurements were compared statistically. The STL files were loaded into 3D evaluation software (Geomagic Design X™ 2013, Geomagic, Morrisville, USA). By using the ‘best-fit algorithm’ method of the comparison software, all data-sets were superimposed. After the best fit superimposition, a more accurate superimposition of the bars were done using the “GLOBAL and FINE and PARTIAL” alignment method in the geomagic software. (Fig. 37,38)

This alignment simulated the “Sheffield Test” or the ‘One-screw Test’ in the software.

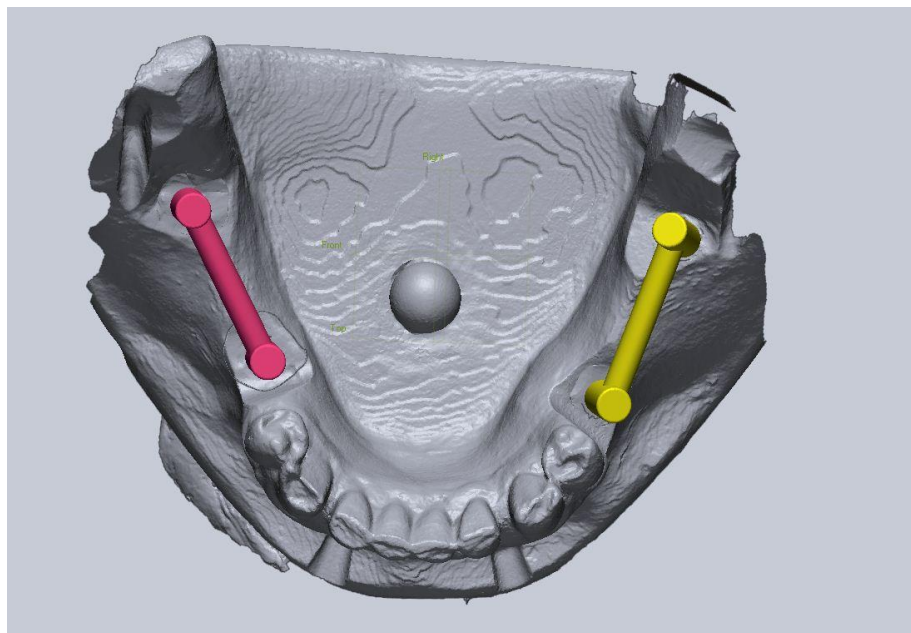


Figure 36: Computer Aided Design of the bars made on parallel (pink) and divergent(yellow) implants.

### **2.3 Data Collection Process:**

The distance measurement between the two center of the control bar was done with all the test bars. There were a total of 4 control bars.

1. Encode Parallel control bar
2. Zirkonzahn Parallel control bar
3. Encode Divergent control bar
4. Zirkonzahn Divergent control bar

The centers of the abutment cylinder bases were marked using the Geomagic Design X Software. The test bars were superimposed on their respective control bars to make the measurement and virtual ‘one-screw test’.

As per the ‘One-Screw Test’ described by White in 1991, one screw was tightened at one terminal abutment and the discrepancies are observed at the other end. This One-screw test was done virtually by aligning the implant interface of one end of the test bar to the control bar using “GLOBAL and FINE and PARTIAL” alignment method in the Geomagic software. After the ‘one-screw alignment’ was achieved on one side, the measurements were made on the other side. (fig.37). Each alignment was confirmed to be precise. It was noted that centers to the abutment bases of Control and Test bars are not more than  $\pm 5\mu$  away from each other. Also, the data points of alignment on one side had more than 95% superimposition as shown by the histogram. (Fig. 38) The measurements used were absolute values and not positive or negative displacements.

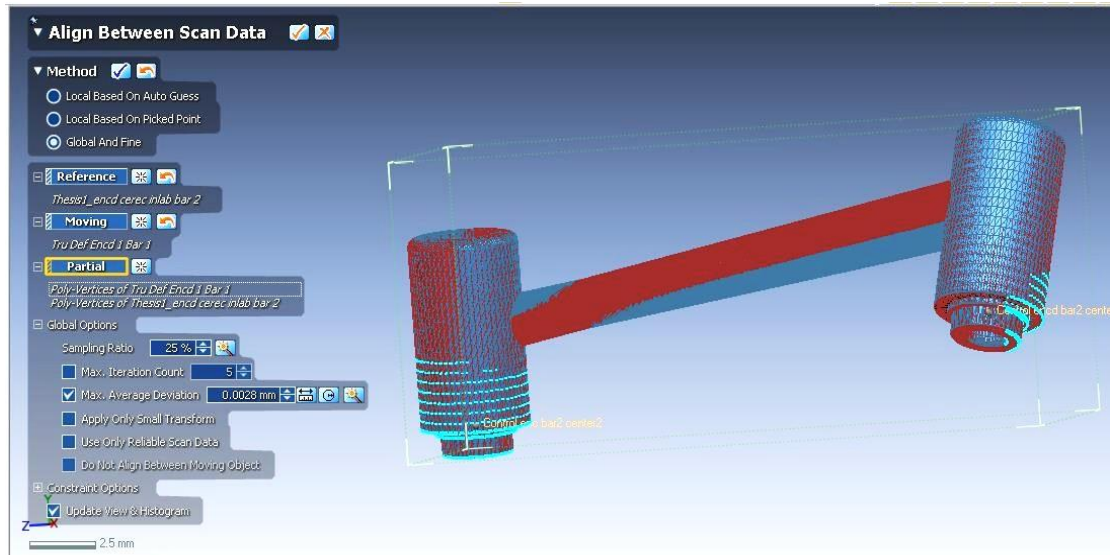


Figure 37: Virtual one-screw test using the Geomagic Desin X. “GLOBAL and FINE and PARTIAL” alignment method. (Light Blue points show the area that is superimposed.)

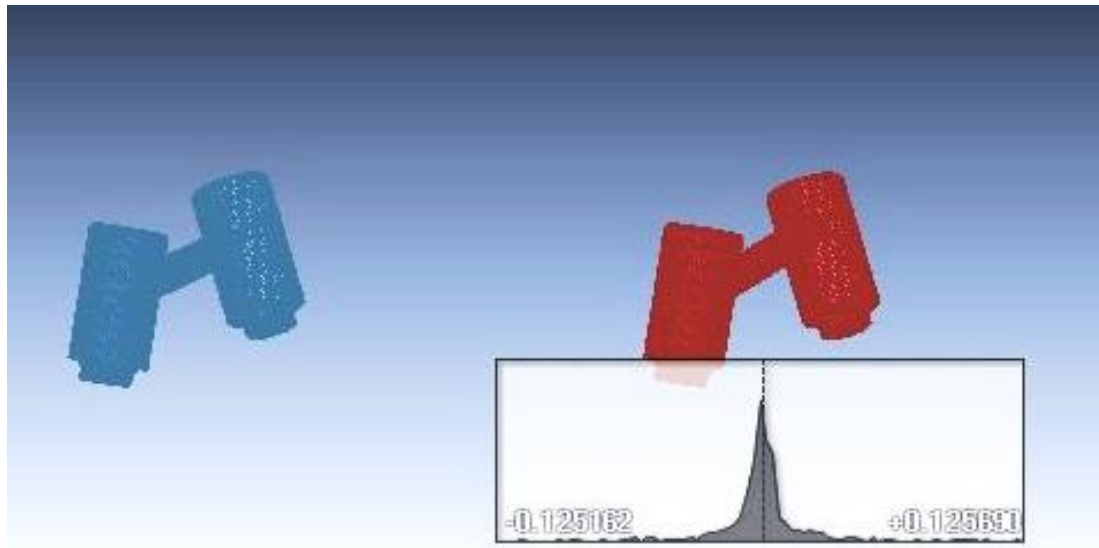


Figure 38: Histogram showing the level of alignment. More than 95% and Less than 5microm gap height on the aligned side.

After the superimposition/alignment was achieved on one of the abutments of the bar between the control and the test scanner, the gap height measurement and planar angle difference measurements were done on the other abutment. To get the gap-height distance (in micrometers) the center points of the control bar and the center point of the test bar were marked at the lesser-superimposed abutment. (Fig. 41-43) The distance between these two center points was measured in microns using the Geomagic Design X<sup>xxxvi</sup> distance measurement tool. This tool in the software can be accessed from the tab Measure>Distance. The default setting of linear distance measurement was done to acquire the distance between the two center points. This distance was designated as the 'gap-height distance' from the implant-abutment interface to the control abutment and the test abutment. (Fig. 42,43)

The planar angle differences were measured by using the plane implant interface of the abutments. This plane was calculated for the control and test bar on the lesser-superimposed abutment. To measure the angle the Measure>Angle tabs were used. The plane-plane angle was measured by clicking the mouse directly on the planes to be measured. Once the plane was determined, their vector angular difference was calculated from the abutment which was closer to the implant. The implant-abutment interface from the lesser-superimposed abutment was again used for getting the angle deviation.(Fig.44,45 )

The final volume measurement was derived from the gap height measurement (Distance between centers) and the angular difference by using a geometrical formula (Fig.46-47).

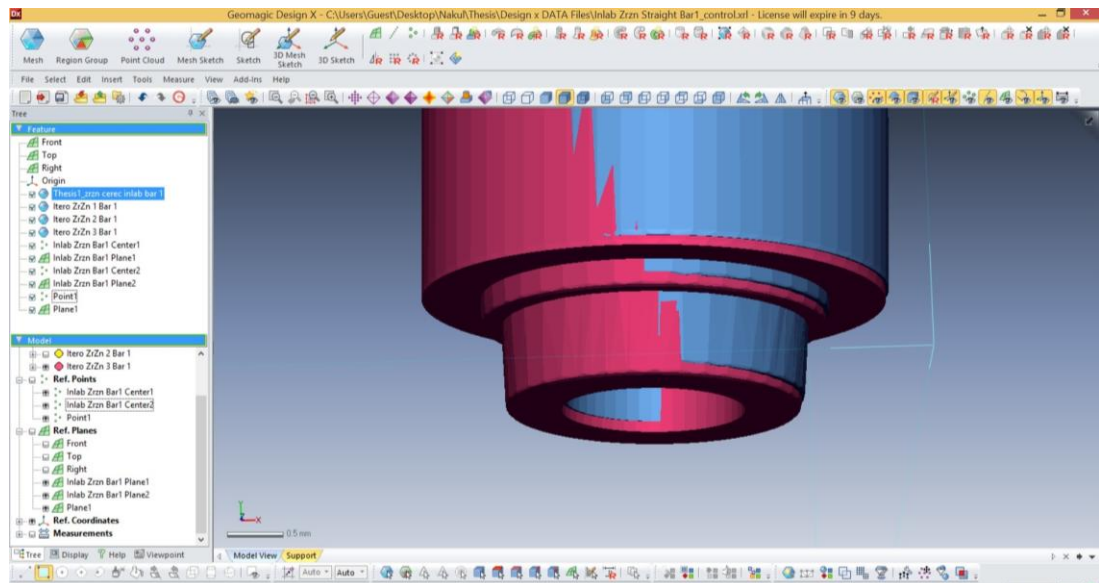


Figure 39: Screenshot of the Geomagic Design X software used for making the virtual measurements.

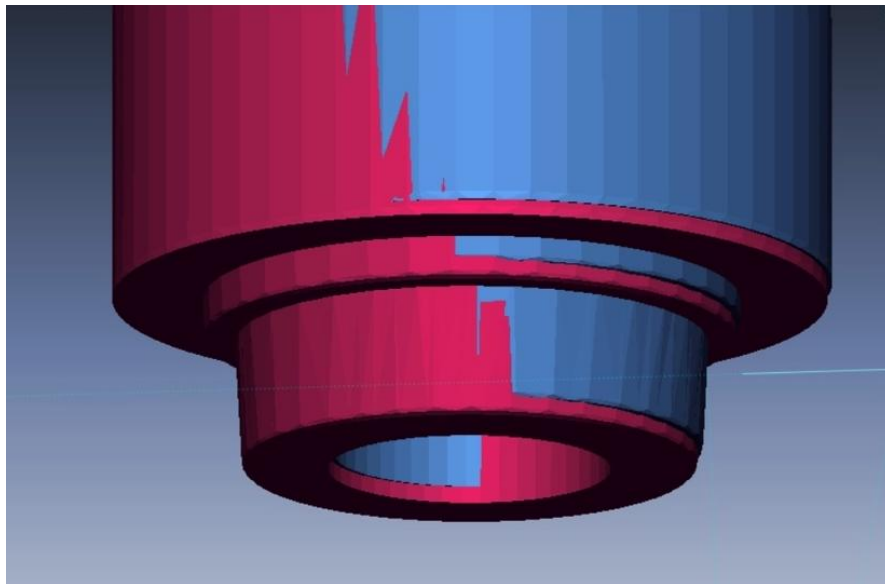


Figure 40: The misfit shown at the control ( Blue) vs the test (Red) abutment.

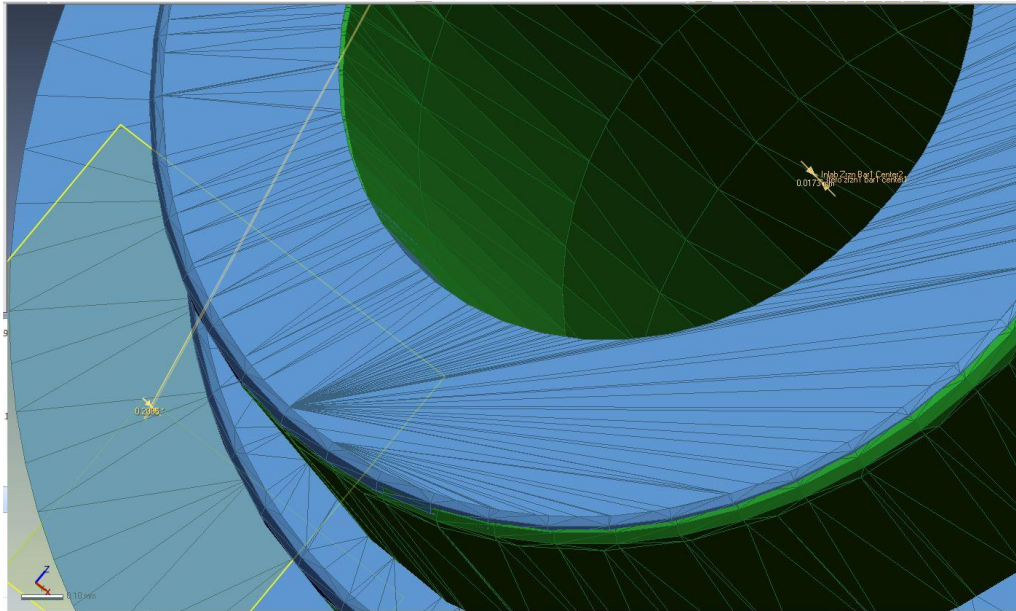


Figure 41: CAD view of the abutment showing the abutment-implant interface where measurements were made. (Blue colored abutment is the Control Abutment and the Green Colored abutment is the Test Abutment)

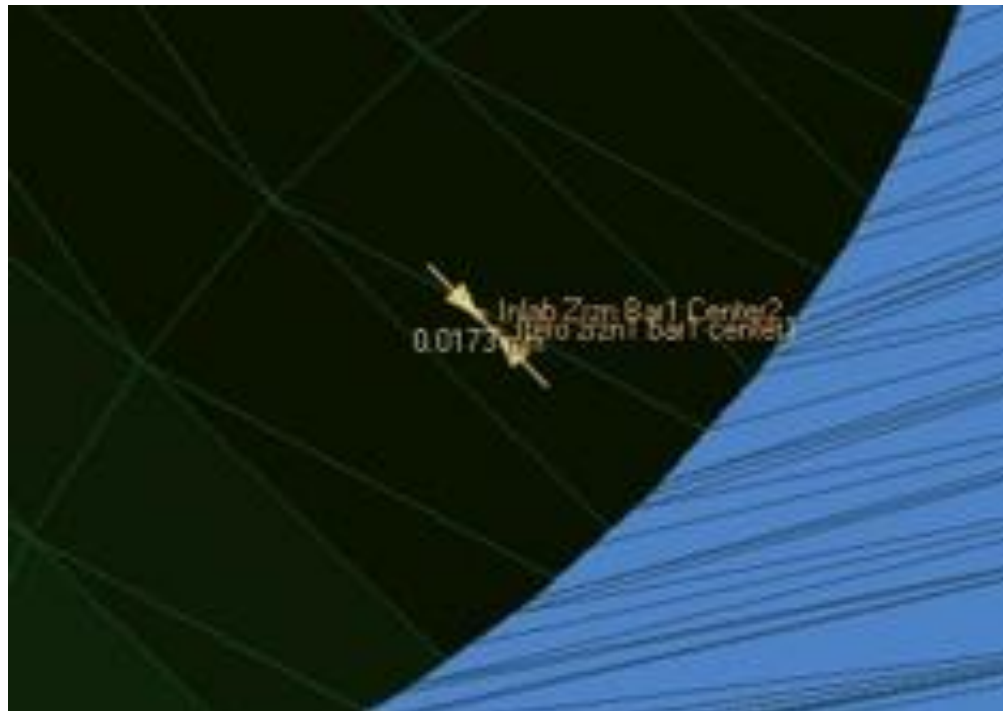


Figure 42: Enlarged view of the center of the abutments showing gap-height measurements being made.

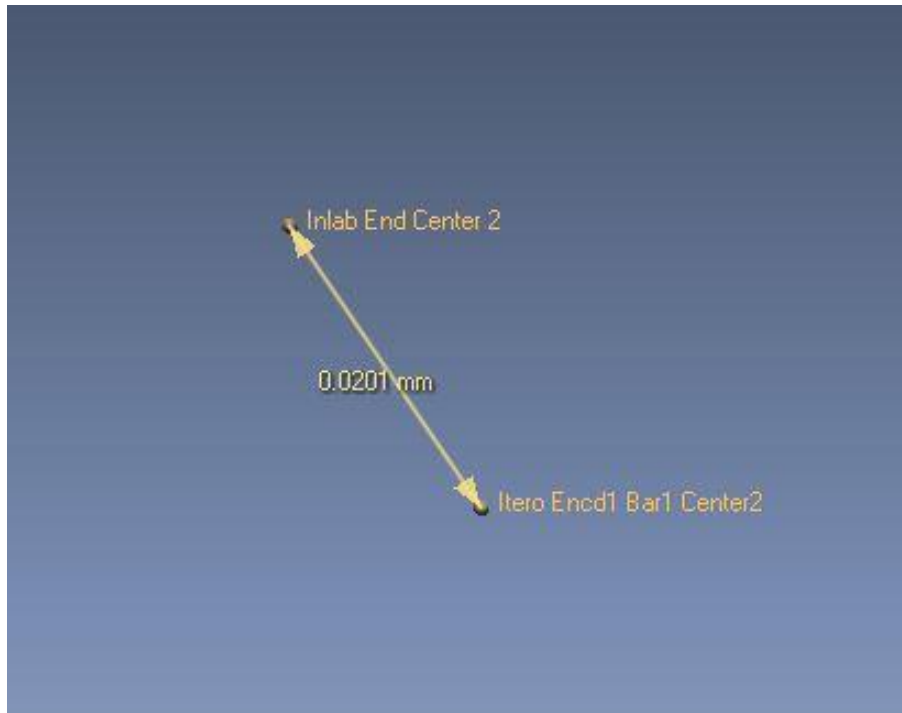


Figure 43: Gap height (distance measurement done between the control and the test )



Figure 44: Enlarged view of the abutment showing the abutment implant interface where the angle deviation measurements were made.

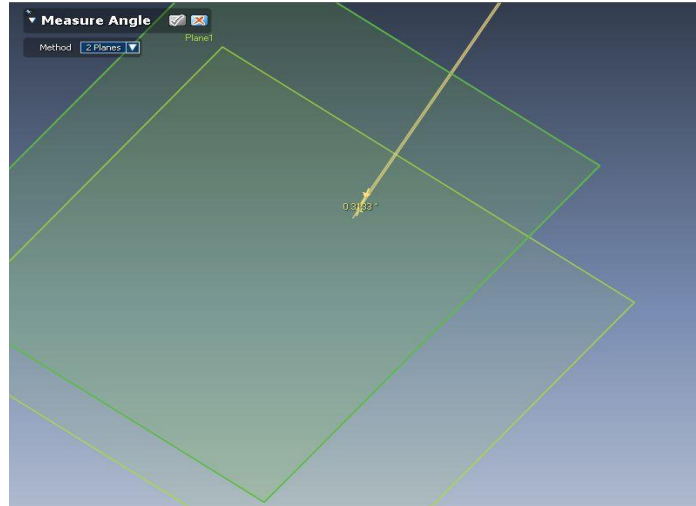


Figure 45: Planar angular difference measurement done between the control and the test

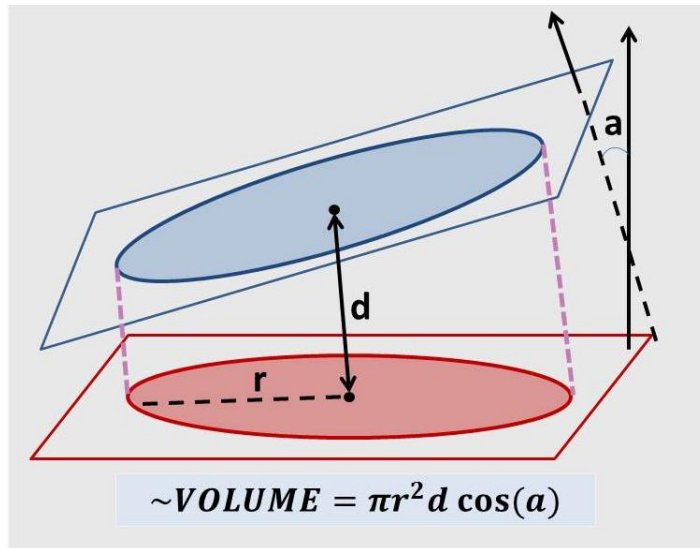


Figure 46: Diagrammatic representation of the Volume misfit.

**Volume of Space**  
Between Bar Platform  
 **$\sim \text{Volume} = \text{Pi} * r^2 * d \cos(a)$**   
where r=radius of platform =2mm  
d=distance  
a=angle between planes

Figure 47: Geometrical formula used for calculating the approximate value of the volume misfit.

#### **2.4 Data Evaluation and Statistical Analysis**

The calculated volume in millimeter cube was analyzed using repeated-measures multifactorial ANOVA and Tukey-test, with a non-directional alpha of 0.05.

A Post-hoc comparison was done showing all the possible combination of the variable types.

#### **2.5 Comparison of Virtual Test with CAM-Titanium Bars**

Four CAD-CAM bars (Fig.30,31,32 ) were obtained from the 40 bars that were designed.

Two bars were from the Control Laboratory Scanner and One from the largest gap-height distance and One from the least gap height distance from the Test Scanners. The actual Sheffield Test<sup>xxxi</sup> was done on the stereolithic model by three investigators.

The four milled Bars were:

1. Control Scanner (Sirona inEos. X5) with Encode Healing Abutment and parallel implants
2. Control Scanner (Sirona inEos. X5) with Zirkozahn Scan Abutment and divergent implants

3. Test Scanner (3M True Definition Scanner) with Zirkonzahn Scan Abutment and parallel implants.(Fig.48)
4. Test Scanner (3Shape Trios Scanner) with Zirkonzahn Scan Abutment and parallel implants.

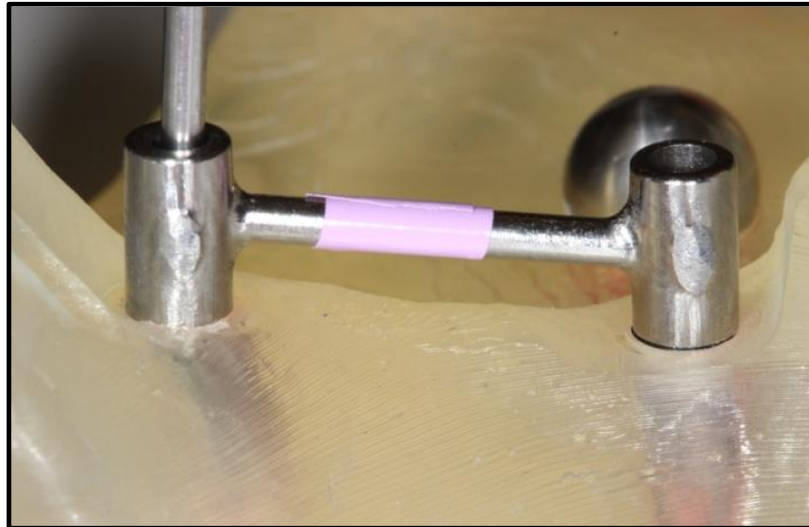


Figure 48: Titanium CAD-CAM Bars used for doing Sheffield Test (One-Screw Test)

## Chapter 3: Results

### 3.1 Abbreviations Used

ENC	Bellatek Encode Healing Abutment
ZRZ	Zirkon Zahn Scan body for Biomet 3i, Certain Prevail implant
P	Parallel Implant
D	Non Parallel or Divergent Implants
TRU	3M LAVA True Definition Scanner
TRI	3Shape Trios Scanner
ITR	Cadent iTero Scanner
SCANBD	Scan Body or Scannable Abutment
DRAW	Implant Angulation or Draw
SCANR	Test Scanner
DIST	Gap Height or Gap Distance (in micrometers or microns).
ANGL	Planar Angular Difference (in degree)
VMIS	Volume Misfit (in millimeter cube)

The volumetric misfit of each of the 36 computer aided designed bars made from the three different scanner, two scannable abutments and two angular variation were calculated. (Table.5)

The results of the gap-height distance and angular deviation between the test bars and their respective controls are presented. (Table.4)

Table 4: Gap-Height Distance and Angle Deviation Data

TRIAL	SCANBD	DRAW	SCANR	DIST (micrn)	ANGL (deg)
1	ENC	P	TRU	12.4000	0.5704
2	ENC	P	TRU	17.1000	0.3424
3	ENC	P	TRU	44.9000	0.4338
4	ENC	P	TRI	75.9000	0.6147
5	ENC	P	TRI	30.9000	0.9278
6	ENC	P	TRI	16.5000	0.5157
7	ENC	P	ITR	20.1000	0.1795
8	ENC	P	ITR	65.7000	0.3507
9	ENC	P	ITR	90.1000	0.2932
10	ZRZ	P	TRU	59.1000	0.1040
11	ZRZ	P	TRU	88.2000	0.0767
12	ZRZ	P	TRU	75.3000	0.1082
13	ZRZ	P	TRI	31.4000	0.4060
14	ZRZ	P	TRI	34.6000	1.2650
15	ZRZ	P	TRI	32.7000	0.1068
16	ZRZ	P	ITR	23.1000	0.1620
17	ZRZ	P	ITR	12.3000	0.0760
18	ZRZ	P	ITR	30.5000	0.3430
19	ENC	D	TRU	30.6000	0.1379
20	ENC	D	TRU	26.1000	0.2704
21	ENC	D	TRU	47.1000	0.2383
22	ENC	D	TRI	64.1000	1.1206
23	ENC	D	TRI	37.5000	0.9528
24	ENC	D	TRI	40.7000	1.0523
25	ENC	D	ITR	42.5000	0.3981
26	ENC	D	ITR	23.4000	0.3790
27	ENC	D	ITR	55.3000	0.3220
28	ZRZ	D	TRU	23.8000	0.1605
29	ZRZ	D	TRU	22.3000	0.2464
30	ZRZ	D	TRU	31.6000	0.3624
31	ZRZ	D	TRI	49.2000	0.9703
32	ZRZ	D	TRI	65.1000	0.9600
33	ZRZ	D	TRI	80.9000	1.2315
34	ZRZ	D	ITR	87.1000	0.2467
35	ZRZ	D	ITR	30.6000	0.1976
36	ZRZ	D	ITR	31.6000	0.1318

Table 5: Volume Deviation Data

TRIAL	SCANBD	DRAW	SCANR	VMIS (mm <sup>3</sup> )
1	ENC	P	TRU	0.1312
2	ENC	P	TRU	0.2024
3	ENC	P	TRU	0.5120
4	ENC	P	TRI	0.7792
5	ENC	P	TRI	0.2328
6	ENC	P	TRI	0.1804
7	ENC	P	ITR	0.2485
8	ENC	P	ITR	0.7754
9	ENC	P	ITR	1.0839
10	ZRZ	P	TRU	0.7387
11	ZRZ	P	TRU	1.1051
12	ZRZ	P	TRU	0.9407
13	ZRZ	P	TRI	0.3625
14	ZRZ	P	TRI	0.1309
15	ZRZ	P	TRI	0.4086
16	ZRZ	P	ITR	0.2865
17	ZRZ	P	ITR	0.1541
18	ZRZ	P	ITR	0.3609
19	ENC	D	TRU	0.3809
20	ENC	D	TRU	0.3161
21	ENC	D	TRU	0.5751
22	ENC	D	TRI	0.3505
23	ENC	D	TRI	0.2730
24	ENC	D	TRI	0.2535
25	ENC	D	ITR	0.4923
26	ENC	D	ITR	0.2732
27	ENC	D	ITR	0.6592
28	ZRZ	D	TRU	0.2952
29	ZRZ	D	TRU	0.2718
30	ZRZ	D	TRU	0.3713
31	ZRZ	D	TRI	0.3494
32	ZRZ	D	TRI	0.4692
33	ZRZ	D	TRI	0.3384
34	ZRZ	D	ITR	1.0614
35	ZRZ	D	ITR	0.3770
36	ZRZ	D	ITR	0.3937

Table 6: Summary data

SCANBD	DRAW	SCANR	Variable	N	Mean	Std Dev	Lower 95% CL for Mean	Upper 95% CL for Mean	Minimum	Maximum
ENC	D	ITR	VMIS	3	0.4749	0.1936	-0.0060	0.9558	0.2732	0.6592
			DIST	3	40.4000	16.0533	0.5213	80.2787	23.4	55.3
			ANGL	3	0.3664	0.0396	0.2680	0.4647	0.322	0.3981
		TRI	VMIS	3	0.2923	0.0513	0.1649	0.4198	0.2535	0.3505
			DIST	3	47.4333	14.5222	11.3583	83.5084	37.5	64.1
			ANGL	3	1.0419	0.0844	0.8323	1.2515	0.9528	1.1206
		TRU	VMIS	3	0.4240	0.1348	0.0892	0.7588	0.3161	0.5751
			DIST	3	34.6000	11.0567	7.1337	62.0663	26.1	47.1
			ANGL	3	0.2155	0.0691	0.0438	0.3872	0.1379	0.2704
	P	ITR	VMIS	3	0.7026	0.4224	-0.3468	1.7520	0.2485	1.0839
			DIST	3	58.6333	35.5310	-29.6306	146.8973	20.1	90.1
			ANGL	3	0.2745	0.0871	0.0580	0.4909	0.1795	0.3507
		TRI	VMIS	3	0.3975	0.3316	-0.4263	1.2213	0.1804	0.7792
			DIST	3	41.1000	30.9858	-35.8730	118.0730	16.5	75.9
			ANGL	3	0.6861	0.2151	0.1517	1.2205	0.5157	0.9278
		TRU	VMIS	3	0.2819	0.2025	-0.2211	0.7848	0.1312	0.512
			DIST	3	24.8000	17.5650	-18.8339	68.4339	12.4	44.9
			ANGL	3	0.4489	0.1147	0.1638	0.7339	0.3424	0.5704

Continued...

Table: 6 Continued...

SCANBD	DRAW	SCANR	Variable	N	Mean	Std Dev	Lower 95% CL for Mean	Upper 95% CL for Mean	Minimum	Maximum
ZRZ	D	ITR	VMIS	3	0.6107	0.3904	-0.3591	1.5805	0.377	1.0614
			DIST	3	49.7667	32.3355	-30.5591	130.0925	30.6	87.1
			ANGL	3	0.1920	0.0577	0.0488	0.3352	0.1318	0.2467
		TRI	VMIS	3	0.3857	0.0726	0.2054	0.5659	0.3384	0.4692
			DIST	3	65.0667	15.8500	25.6930	104.4403	49.2	80.9
			ANGL	3	1.0539	0.1539	0.6717	1.4362	0.96	1.2315
		TRU	VMIS	3	0.3128	0.0520	0.1835	0.4420	0.2718	0.3713
			DIST	3	25.9000	4.9930	13.4967	38.3033	22.3	31.6
			ANGL	3	0.2564	0.1013	0.0047	0.5081	0.1605	0.3624
	P	ITR	VMIS	3	0.2672	0.1047	0.0070	0.5274	0.1541	0.3609
			DIST	3	21.9667	9.1528	-0.7701	44.7034	12.3	30.5
			ANGL	3	0.1937	0.1363	-0.1449	0.5322	0.076	0.343
		TRI	VMIS	3	0.3007	0.1488	-0.0690	0.6704	0.1309	0.4086
			DIST	3	32.9000	1.6093	28.9022	36.8978	31.4	34.6
			ANGL	3	0.5926	0.6012	-0.9009	2.0861	0.1068	1.265
		TRU	VMIS	3	0.9282	0.1835	0.4723	1.3841	0.7387	1.1051
			DIST	3	74.2000	14.5812	37.9784	110.4216	59.1	88.2
			ANGL	3	0.0963	0.0171	0.0538	0.1388	0.0767	0.1082

### 3.2 Volume Misfit Results

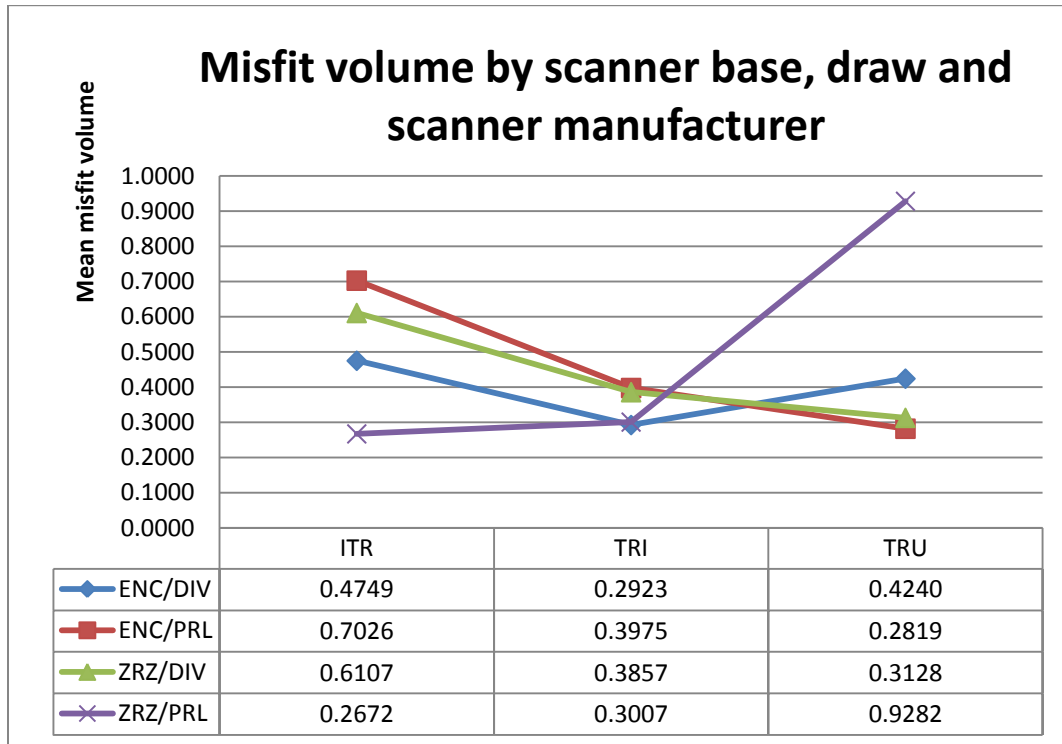


Figure 49: Volume Misfit Results

The volume discrepancy values ranged from 0.1309mm<sup>3</sup> to 1.1051mm<sup>3</sup>. (Table.5)

The most accurate combination for volumetric misfit of 0.1309mm<sup>3</sup> in this study was, 3Shape Trios Scanner used with Zirkozahn Abutments and Parallel implants. The least accurate combination of variables for volumetric misfit of 1.1051mm<sup>3</sup>, according to the results of this study, was the 3M Lava True Definition Scanner used with Zirkozahn Abutments and Parallel implants.

If the ‘Mean Volume Misfit’ of each combination was considered (Table.6), Itero Scanner used with Zirkozahn abutment and Parallel implants had the most accurate result (0.2672mm<sup>3</sup>) and the combination of 3M Lava True Definition with Zirkozahn abutment and Parallel implants had the least accurate mean result (0.9282mm<sup>3</sup>)

### 3.3 Gap-Height Distance Misfit Results:

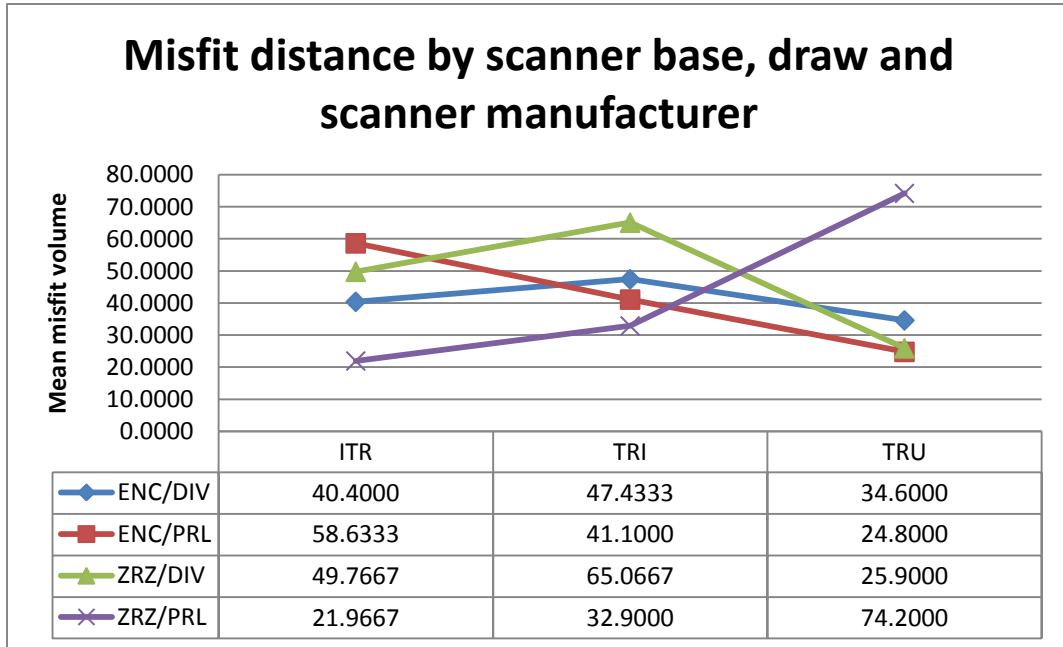


Figure 50: Gap-Height Distance Misfit Results

The gap-height distance value ranges from 12.30  $\mu$  to 90.40  $\mu$  (Table.4)

The most accurate combination for gap-height distance of 12.30  $\mu$  in this study was the Itero Scanner used with Zirkozahn abutment and Parallel implants. The least accurate combination of variables for gap height distance misfit of 90.40 $\mu$  was 3M Lava True Definition Scanner used with Zirkozahn Abutments and Parallel implants.

If the ‘Mean Gap-Height Misfit’ of each combination was considered (Table.6), Itero Scanner used with Zirkozahn abutment and Parallel implants had the most accurate result (Mean = 21.9667 $\mu$ ) and the combination of 3M Lava True Definition with Zirkozahn abutment and Parallel implants had the least accurate mean result (mean=0.9282mm<sup>3</sup>)

### 3.4 Angle Misfit Results :

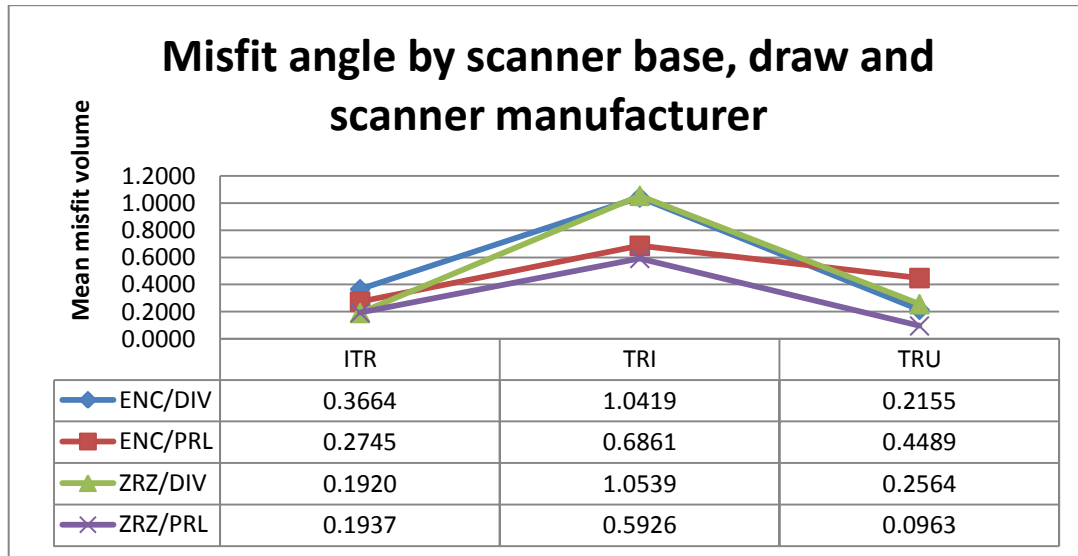


Figure 51: Angle Misfit Results

The angular misfit value ranged from 0.0760° to 1.2650 ° (Table.4).

The most accurate combination for angular misfit of 0.0760° in this study was Itero Scanner used with Zirkonzahn abutment and Parallel implants. The least accurate combination of variables for angular misfit of 1.2650° was the 3shape Trios Scanner used with Zirkonzahn Abutments and Parallel implants.

If the ‘Mean Angular Misfit’ of each combination was considered (Table.6) the 3M Lava True Definition Scanner used with Zirkonzahn abutment and Parallel implants had the most accurate result (mean=0.0963°) and the combination of 3Shape Trios Scanner with Zirkonzahn abutment and 30° divergent implants had the least accurate mean result (mean=1.0539°)

### 3.5 ANOVA Summary:

Table 7: ANOVA summary

<b>Effect</b>	<b>Num DF</b>	<b>Den DF</b>	<b>F Value</b>	<b>Pr &gt; F</b>
SCANBD	1	24	0.39	0.5363
DRAW	1	24	1.04	0.3173
SCANBD*DRAW	1	24	0	0.9919
SCANR	2	24	2.92	0.0731
SCANBD*SCANR	2	24	3.93	0.0334
DRAW*SCANR	2	24	2.09	0.1458
SCANBD*DRAW*SCANR	2	24	10.28	0.0006

The results of the multifactorial ANOVA shows that there was a statistically significant three-way interaction of the variables. (p=0.0006)

None of the three intra-oral scanners tested (3M LAVA True Definition, 3Shape Trios and Cadent iTero) were more accurate than the others under all conditions (p=0.0731).

Neither the Encode nor Zirkonzahn abutments allowed for a more accurate implant impression than the other, under all testing conditions (p=0.5363).

Neither the Parallel implant nor the 30<sup>0</sup> Angled Implant position allowed for a more accurate impression under all testing conditions (p=0.3173).

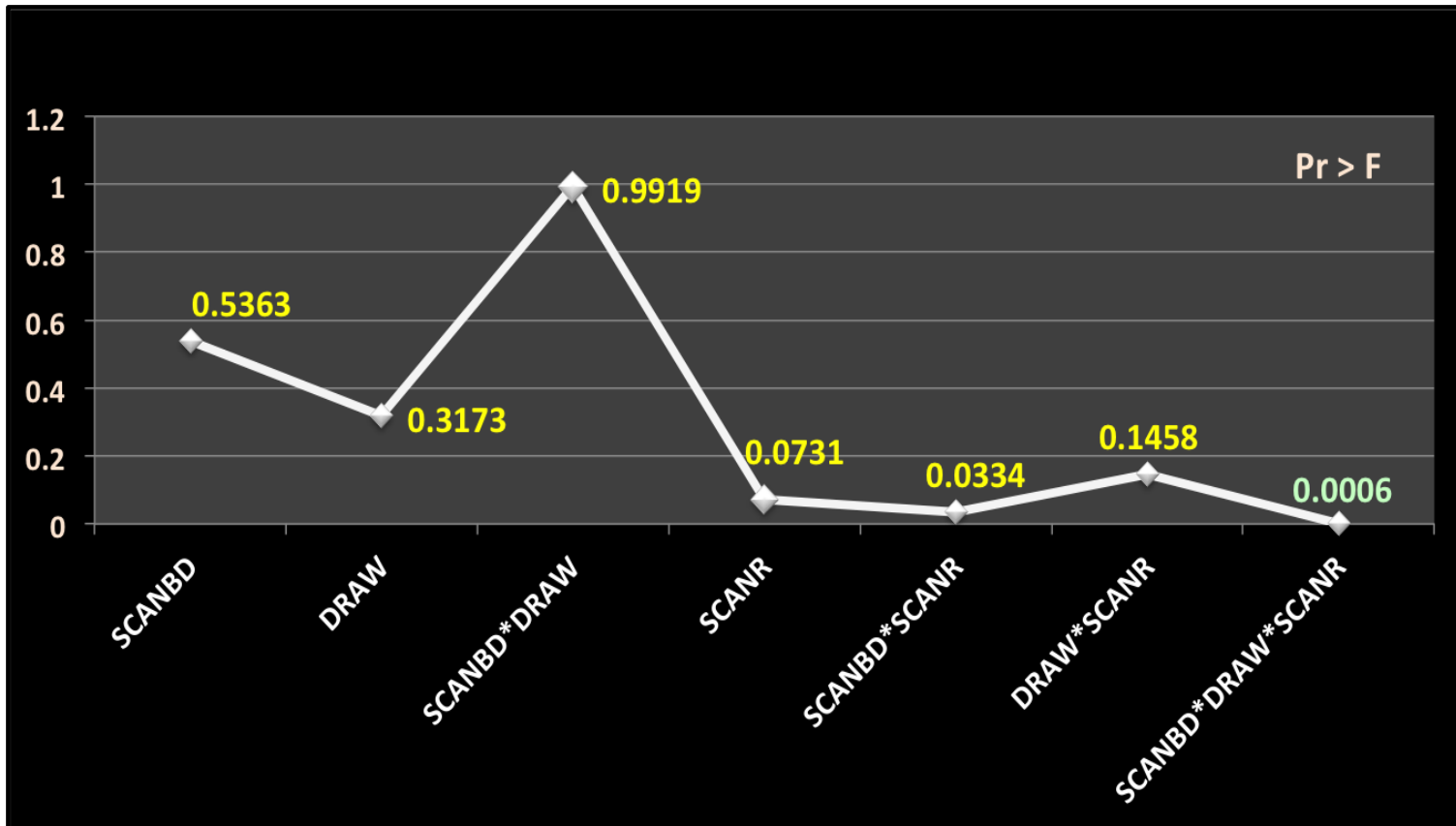


Figure 52: ANOVA Summary

Table 8: Post hoc comparisons

SCANBD	DRAW	SCANR	SCANBD	DRAW	SCANR	Estimate	Standard Error	DF	t Value	Pr >  t	Adjustment	Adj P
ENC	D	ITR	ENC	D	TRU	0.0509	0.1509	24	0.34	0.739	Tukey	1.0000
ENC	D	ITR	ENC	P	ITR	-0.2277	0.1509	24	-1.51	0.1444	Tukey	0.9238
ENC	D	ITR	ENC	P	TRI	0.0774	0.1509	24	0.51	0.6126	Tukey	1.0000
ENC	D	ITR	ENC	P	TRU	0.1930	0.1509	24	1.28	0.2131	Tukey	0.9743
ENC	D	ITR	ZRZ	D	ITR	-0.1358	0.1509	24	-0.9	0.3771	Tukey	0.9985
ENC	D	ITR	ZRZ	D	TRI	0.0892	0.1509	24	0.59	0.5598	Tukey	1.0000
ENC	D	ITR	ZRZ	D	TRU	0.1621	0.1509	24	1.07	0.2933	Tukey	0.9931
ENC	D	ITR	ZRZ	P	ITR	0.2077	0.1509	24	1.38	0.1814	Tukey	0.9574
ENC	D	ITR	ZRZ	P	TRI	0.1742	0.1509	24	1.15	0.2596	Tukey	0.9879
ENC	D	ITR	ZRZ	P	TRU	-0.4533	0.1509	24	-3	0.0062	Tukey	0.1679
ENC	D	TRI	ENC	D	TRU	-0.1317	0.1509	24	-0.87	0.3915	Tukey	0.9988
ENC	D	TRI	ENC	P	ITR	-0.4103	0.1509	24	-2.72	0.012	Tukey	0.2754
ENC	D	TRI	ENC	P	TRI	-0.1051	0.1509	24	-0.7	0.4927	Tukey	0.9999
ENC	D	TRI	ENC	P	TRU	0.0105	0.1509	24	0.07	0.9453	Tukey	1.0000
ENC	D	TRI	ZRZ	D	ITR	-0.3184	0.1509	24	-2.11	0.0455	Tukey	0.6213
ENC	D	TRI	ZRZ	D	TRI	-0.0933	0.1509	24	-0.62	0.5421	Tukey	1.0000
ENC	D	TRI	ZRZ	D	TRU	-0.0204	0.1509	24	-0.14	0.8934	Tukey	1.0000
ENC	D	TRI	ZRZ	P	ITR	0.0252	0.1509	24	0.17	0.8689	Tukey	1.0000
ENC	D	TRI	ZRZ	P	TRI	-0.0083	0.1509	24	-0.06	0.9564	Tukey	1.0000
ENC	D	TRI	ZRZ	P	TRU	-0.6358	0.1509	24	-4.21	0.0003	Tukey	0.0127
ENC	D	TRU	ENC	P	ITR	-0.2786	0.1509	24	-1.85	0.0773	Tukey	0.7786
ENC	D	TRU	ENC	P	TRI	0.0266	0.1509	24	0.18	0.8617	Tukey	1.0000
ENC	D	TRU	ENC	P	TRU	0.1422	0.1509	24	0.94	0.3555	Tukey	0.9977
ENC	D	TRU	ZRZ	D	ITR	-0.1867	0.1509	24	-1.24	0.2281	Tukey	0.9798
ENC	D	TRU	ZRZ	D	TRI	0.0384	0.1509	24	0.25	0.8015	Tukey	1.0000
ENC	D	TRU	ZRZ	D	TRU	0.1113	0.1509	24	0.74	0.4681	Tukey	0.9998
ENC	D	TRU	ZRZ	P	ITR	0.1569	0.1509	24	1.04	0.3089	Tukey	0.9948

Continued...

Table: 8 Continued...

SCANBD	DRAW	SCANR	SCANBD	DRAW	SCANR	Estimate	Standard Error	DF	t Value	Pr >  t	Adjustment	Adj P
ENC	D	TRU	ZRZ	P	TRI	0.1234	0.1509	24	0.82	0.4217	Tukey	0.9994
ENC	D	TRU	ZRZ	P	TRU	-0.5041	0.1509	24	-3.34	0.0027	Tukey	0.0872
ENC	P	ITR	ENC	P	TRI	0.3051	0.1509	24	2.02	0.0545	Tukey	0.6759
ENC	P	ITR	ENC	P	TRU	0.4207	0.1509	24	2.79	0.0102	Tukey	0.2456
ENC	P	ITR	ZRZ	D	ITR	0.0919	0.1509	24	0.61	0.5483	Tukey	1.0000
ENC	P	ITR	ZRZ	D	TRI	0.3169	0.1509	24	2.1	0.0464	Tukey	0.6273
ENC	P	ITR	ZRZ	D	TRU	0.3898	0.1509	24	2.58	0.0163	Tukey	0.3406
ENC	P	ITR	ZRZ	P	ITR	0.4354	0.1509	24	2.89	0.0081	Tukey	0.2077
ENC	P	ITR	ZRZ	P	TRI	0.4019	0.1509	24	2.66	0.0136	Tukey	0.3009
ENC	P	ITR	ZRZ	P	TRU	-0.2256	0.1509	24	-1.49	0.148	Tukey	0.9281
ENC	P	TRI	ENC	P	TRU	0.1156	0.1509	24	0.77	0.4511	Tukey	0.9996
ENC	P	TRI	ZRZ	D	ITR	-0.2132	0.1509	24	-1.41	0.1705	Tukey	0.9495
ENC	P	TRI	ZRZ	D	TRI	0.0118	0.1509	24	0.08	0.9383	Tukey	1.0000
ENC	P	TRI	ZRZ	D	TRU	0.0847	0.1509	24	0.56	0.5798	Tukey	1.0000
ENC	P	TRI	ZRZ	P	ITR	0.1303	0.1509	24	0.86	0.3964	Tukey	0.9989
ENC	P	TRI	ZRZ	P	TRI	0.0968	0.1509	24	0.64	0.5273	Tukey	0.9999
ENC	P	TRI	ZRZ	P	TRU	-0.5307	0.1509	24	-3.52	0.0018	Tukey	0.0605
ENC	P	TRU	ZRZ	D	ITR	-0.3288	0.1509	24	-2.18	0.0394	Tukey	0.5777
ENC	P	TRU	ZRZ	D	TRI	-0.1038	0.1509	24	-0.69	0.4981	Tukey	0.9999
ENC	P	TRU	ZRZ	D	TRU	-0.0309	0.1509	24	-0.2	0.8395	Tukey	1.0000
ENC	P	TRU	ZRZ	P	ITR	0.0147	0.1509	24	0.1	0.9232	Tukey	1.0000
ENC	P	TRU	ZRZ	P	TRI	-0.0188	0.1509	24	-0.12	0.9019	Tukey	1.0000
ENC	P	TRU	ZRZ	P	TRU	-0.6463	0.1509	24	-4.28	0.0003	Tukey	0.0108
ZRZ	D	ITR	ZRZ	D	TRI	0.2250	0.1509	24	1.49	0.1489	Tukey	0.9291
ZRZ	D	ITR	ZRZ	D	TRU	0.2979	0.1509	24	1.97	0.06	Tukey	0.7049
ZRZ	D	ITR	ZRZ	P	ITR	0.3435	0.1509	24	2.28	0.032	Tukey	0.5167
ZRZ	D	ITR	ZRZ	P	TRI	0.3100	0.1509	24	2.05	0.051	Tukey	0.6558
ZRZ	D	ITR	ZRZ	P	TRU	-0.3175	0.1509	24	-2.1	0.0461	Tukey	0.6251

52

Continued...

Table: 8 Continued...

SCANBD	DRAW	SCANR	SCANBD	DRAW	SCANR	Estimate	Standard Error	DF	t Value	Pr >  t	Adjustment	Adj P
ZRZ	D	TRI	ZRZ	D	TRU	0.0729	0.1509	24	0.48	0.6334	Tukey	1.0000
ZRZ	D	TRI	ZRZ	P	ITR	0.1185	0.1509	24	0.79	0.44	Tukey	0.9996
ZRZ	D	TRI	ZRZ	P	TRI	0.0850	0.1509	24	0.56	0.5785	Tukey	1.0000
ZRZ	D	TRI	ZRZ	P	TRU	-0.5425	0.1509	24	-3.59	0.0015	Tukey	0.0512
ZRZ	D	TRU	ZRZ	P	ITR	0.0456	0.1509	24	0.3	0.7651	Tukey	1.0000
ZRZ	D	TRU	ZRZ	P	TRI	0.0121	0.1509	24	0.08	0.9368	Tukey	1.0000
ZRZ	D	TRU	ZRZ	P	TRU	-0.6154	0.1509	24	-4.08	0.0004	Tukey	0.0174
ZRZ	P	ITR	ZRZ	P	TRI	-0.0335	0.1509	24	-0.22	0.8262	Tukey	1.0000
ZRZ	P	ITR	ZRZ	P	TRU	-0.6610	0.1509	24	-4.38	0.0002	Tukey	0.0086
ZRZ	P	TRI	ZRZ	P	TRU	-0.6275	0.1509	24	-4.16	0.0004	Tukey	0.0145

### **3.6 Results of the Post-hoc analysis**

1. The combination of Encode Healing Abutment used with divergent implants and 3Shape -Trios scanner (mean=0.29mm<sup>3</sup>) was significantly more accurate than the Zirkonzahn Scan body used with parallel implant and 3M-True Definition scanner (mean=0.92mm<sup>3</sup>) [P=0.01].
2. The combination of Encode Healing Abutment used with parallel implants and 3M-True Definition scanner (mean=0.28mm<sup>3</sup>) was significantly more accurate than the Zirkonzahn Scan body used with parallel implant and 3M-True Definition scanner (mean=0.92mm<sup>3</sup>) [P=0.01].
3. The combination of Zirkonzahn Scan body used with divergent implants and 3M-True Definition scanner (mean=0.31mm<sup>3</sup>) was significantly more accurate than the Zirkonzahn Scan body used with parallel implant and 3M-True Definition scanner (mean=0.92mm<sup>3</sup>) [P=0.01].
4. The combination of Zirkonzahn Scan body used with parallel implants and Cadent iTero scanner (mean=0.27mm<sup>3</sup>) was significantly more accurate than the Zirkonzahn Scan body used with Parallel implant and 3M-True Definition scanner (mean=0.92mm<sup>3</sup>) [P=0.01].
5. The combination of Zirkonzahn Scan body used with parallel implant and 3Shape -Trios scanner (mean=0.30mm<sup>3</sup>) was significantly more accurate than the Zirkonzahn Scan body used with Parallel implant and 3M-True Definition scanner (mean=0.92mm<sup>3</sup>) [P=0.01].

### 3.7 Results of Sheffield Test (One Screw Test) of the Milled bars

1. The assessment from all three investigators showed that the fit of all bars except the one made from Test Scanner (3M True Definition Scanner) with Zirkonzahn Scan Abutment and parallel implants did not have a detectable misfit. (Fig. 53,54)
2. The bar made from Test Scanner (3M True Definition Scanner) with Zirkonzahn Scan Abutment and parallel implants which showed a misfit of about  $3/8^{\text{th}}$  of a turn (Fig. 55, 56) after initial resistance was felt.

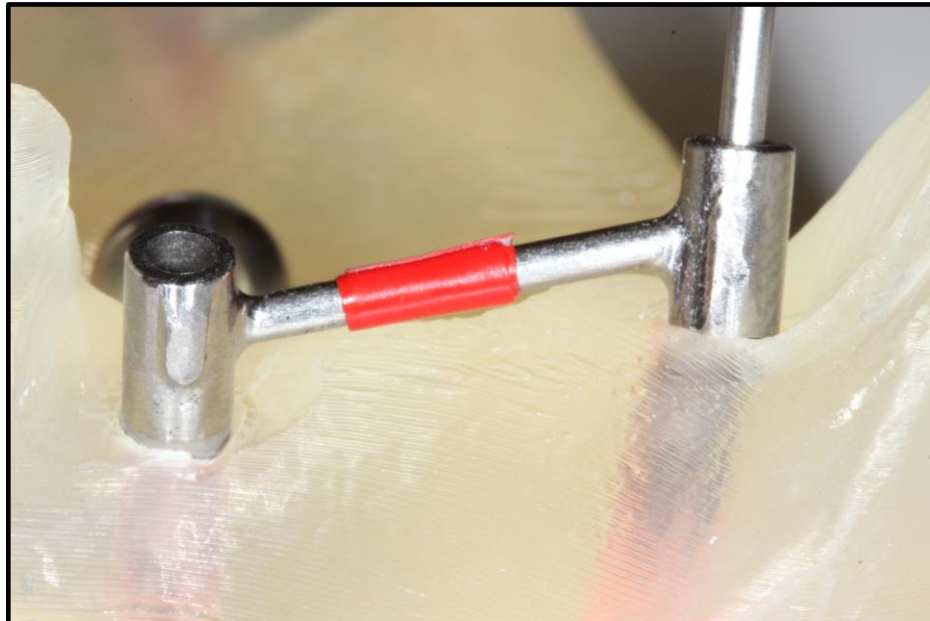


Figure 53. Actual CAD-CAM Bar one-screw test with good fit.



Figure 54: Close-up view of the precisely fitting bar made from the Control Scanner

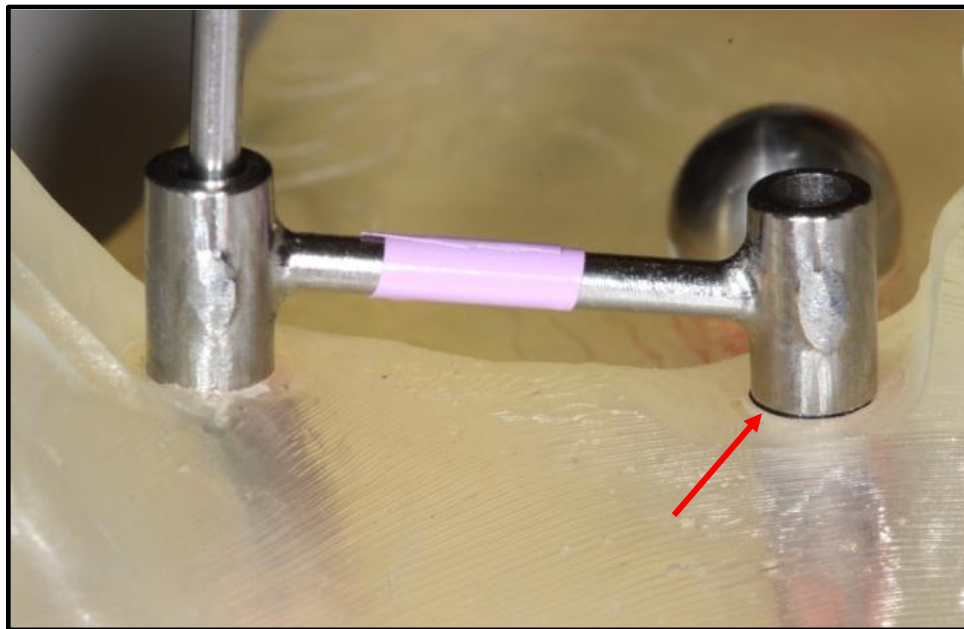


Figure 55: Actual CAD-CAM Bar one-screw test showing the gap



Figure 56: Close-up view of the Gap height difference noted in the bar made from the least accurate designed bar as per the CAD assessment.

## Chapter 4: Discussion

This study was designed to evaluate the accuracy of intra-oral scanners for implant impressions with various scanning systems, scannable abutments and angular variation. The three null hypotheses that were tested in the study were rejected because significant difference in the volume misfit was noted. This difference was noted when the three way interaction between the independent variables was checked. The use of Geomagic Design X software for the virtual one screw test was an interesting finding from the study. Using this method can selectively align data in the software and permit multiple analyses. Since the fit of the bar that was milled with the 88.20 micron inaccuracy showed similar misfit, it suggests that this virtual testing can be used for doing more prosthesis fit related studies. The actual misfit was checked visually and also with a physical one screw test and also screw resistance test described by Jemt (1991)<sup>xxix</sup>. Half a turn of the screw after the first point of resistance meant 180° turn, which was half the pitch of the prosthetic gold screw. The pitch of the prosthetic screw was 300μ, so half is 150μ. The ability to close a gap of 150μ under 15Ncm torque may be an acceptable gauge for fit versus misfit. (Fig.57)



Figure 57: Clinical Situation showing a one screw test.

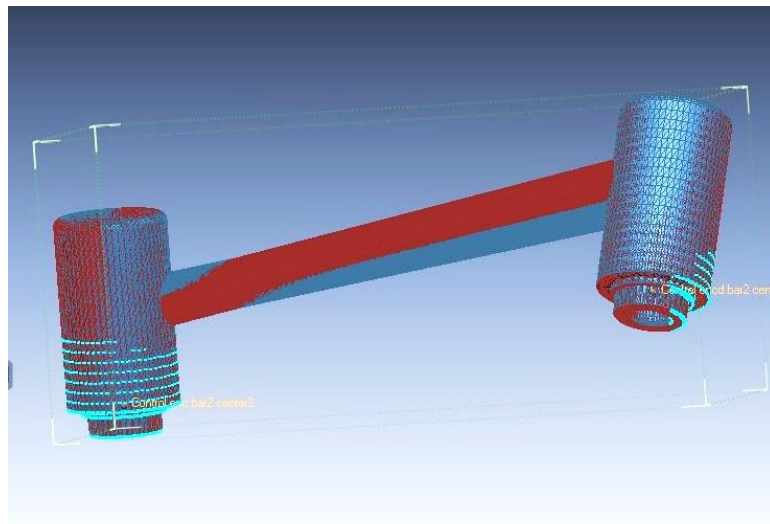


Figure 58: Virtual One-Screw Test Done on Geomagic Design X

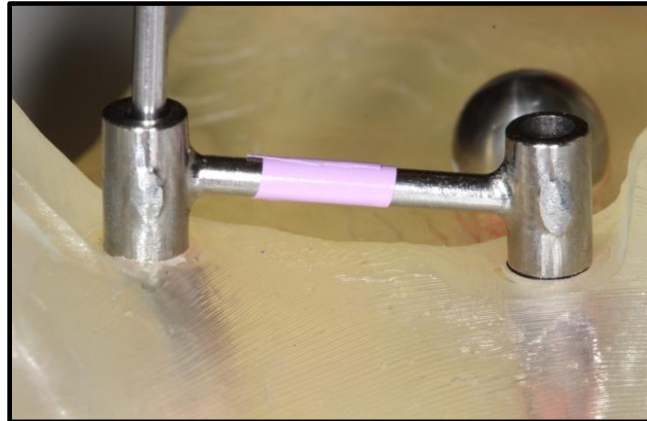


Figure 59: Actual CAD-CAM Bar one-screw test showing the gap

The fit of the prosthesis is important both for the biologic health of the implants and the prosthetic complication.(Fig.57) The stress and strain (Clelland et al <sup>xxxvii</sup>) on the prosthetic screw was less when the prosthesis was passively fitting. According to Jemt et al<sup>xxxix</sup> in 1991, a misfit of 111  $\mu$  did not show any biological implications and the empirical half turn, which amounts to 150 $\mu$ , was also clinically acceptable. Kan et al (1999)<sup>xxx</sup> in their review about the clinical assessment of implant misfit, showed no conclusive number telling the perfect cut-off line for judging implant framework misfits (but most of them were in the 90 to 275 micron range). So, according to that data, all the prostheses designed from all the scanners tested in this study showed a clinically acceptable fit of the implant FPD.(Fig. 58, 59) This suggests that intra-oral scanners, which have completely different technologies and methods of data procurement, all show acceptable accuracy to fabricate screw retained, short-span implant prostheses.

These intra-oral scanners have been tested for accuracy for making inlays, onlays and crowns and other restorative work. The results from this study, to check the impression

achieved after the virtual analogues were placed and prosthesis designed, were very close to the inaccuracies noted by Syrek et al. 2010.<sup>xxvi</sup> Their study done with the 3M LAVA COS showed a marginal gap of 49 $\mu$ , which was very similar to the 3M LAVA True Definition which is the newer model for the same company (but using the same active waveform sampling technology). Results of the study demonstrated that the accuracy of the intra-oral scanning systems for short span implant supported fixed partial dentures was comparable to intra-oral scanning for restorative dentistry on teeth.

The data of the Howell et al<sup>xvi</sup> and Eliasson et al<sup>xviii</sup> studies on VPS impressions of the Encode and the Robocast technique showed significantly less accurate casts made from Robocast as compared to the conventional open and closed tray techniques. The data from Howell et al (Table.7) showed that the accuracy of closed tray and open tray were in the same range of 19 $\mu$  to 54  $\mu$  and the mean IOS impressions accuracy ranged from 21 $\mu$  to 74 $\mu$ . This suggests that IOS accuracy is very close to the conventional Open Tray and Closed Tray impression technique range.(Gap Height Discrepancy)

Table 9: Howell et al data of the same model with conventional impression techniques<sup>xvi</sup>

	Closed		Open	
	Mean Difference ( $\mu$ m)	S.Dev	Mean Difference ( $\mu$ m)	S. Dev
Non-Parallel	<b>54.7</b>	59.5	<b>49.6</b>	57.8
Parallel	<b>34.9</b>	22.1	<b>19.3</b>	19.6

The different designs of the scanable abutments also did not make much difference. As long as there is enough data to superimpose and align the library file and the scan of the abutment the design of the abutment, it seemed that no difference was noted. One might have expected that the bigger scan abutment could have performed better (Zirkonzahn), since it had more data points to align the data, but according to the results of this study it did not make a difference.

The angle differences ranged from all  $0.07^{\circ}$  to  $1.2^{\circ}$  deviation which compared favorably to the data from Eliasson et al<sup>xviii</sup> which showed angle deviation range of  $0.11^{\circ}$  to  $0.89^{\circ}$  for conventional open tray technique and  $0.37^{\circ}$  to  $.42^{\circ}$  deviation range for Robocast technique of Encode. These comparisons suggest that the IOS did give comparable results for the angle deviation, as well, from  $0.09^{\circ}$  to  $1.05^{\circ}$ .

There are advantages of using IOS impressions and a complete CAD-CAM protocol for the fabrication of implant prosthesis. The process becomes more predictable and efficient removing the possible human errors in the manual fabrication process. Also it eliminates many of the material errors that appear during processing. This fact, from a commercial dental laboratory's perspective, would be an efficient way to manage quality consistency. There are a lot of new materials that are be introduced and have the potential to be milled and 3D Printed and so growth in this area is promising.

There are a few concerns as well, which should not be neglected when talking about these intra-oral scanners for implant prostheses. All implant systems do not have scannable abutments that can be used in the patient's mouth. So scanning intra-orally is not always possible. There is mixed review and data about the use of IOS for full arch implant

prosthesis and more research is needed in that direction. Although the prices of these scanners have come down significantly, they are still an expensive equipment to buy and maintain.

As per the Sheffield test described by White et al<sup>xxxi</sup>, one screw is tightened at one terminal abutment and the discrepancies are observed at the other end. The 1-screw test can be used in conjunction with direct vision and explorer when the margins are supragingival or with periapical radiographs when the margins are subgingival. However, the discrepancies are often masked if the distortion has occurred in the negative direction which results in a “bottoming out” phenomenon.<sup>xxix xxx</sup> Therefore, the one-screw test needs to be performed on both the abutments in a two implant FDP. This study used the concept of the one screw test to check the accuracy of the fit of the bar but the absolute value of the height discrepancy was considered instead of performing the virtual one-screw test on both abutments.

Within the limitations of the study, an assessment can be made that IOS can be used for doing implant impressions for fabrication of single tooth to short span FDP's, but there is a need of more quantitative comparison of the CAD assessment versus the milled Bars that are made from that scan. Also, since the study was performed on stereolithic model which was translucent, a contrast powder had to be used during impressions with the scanners that normally do not need powder. Future clinical studies are needed to assess the efficacy of these IOS systems in patients. Also, there are other scanning systems available too, which can be added to future analysis.

## Chapter 5: Conclusion

1. Geomagic Design X software analysis showed a similar virtual misfit to the actual physical misfit observed in fabricated milled bars, therefore the *virtual one-screw test* and design analysis of dental CAD-CAM prosthesis is a viable alternative for research in this area.
2. None of the three intra-oral scanners tested, 3M LAVA True Definition, 3Shape Trios and Cadent iTero were more accurate than the others under all conditions ( $p=0.0731$ ).
3. Neither the Encode nor Zirkozahn abutments allowed for a more accurate implant impression than the other under all testing conditions ( $p=0.5363$ ).
4. Neither the Parallel implant nor the  $30^{\circ}$  Angled Implant position allowed for a more accurate impression under all testing conditions ( $p=0.3173$ ).
5. The combination of Zirkozahn Scan body used with parallel implants and Cadent iTero scanner (mean= $0.27\text{mm}^3$ ) was most accurate and combination of Zirkozahn Scan body used with Parallel implant and 3M-True Definition scanner was the least accurate. (mean= $0.92\text{mm}^3$ )
6. The CAD-CAM prosthesis from the intra-oral scans had a misfit range of  $12.40\ \mu$

to 90.20 $\mu$ , all of which would remain in the clinically acceptable range.

7. This information suggests that intra-oral scans can be used for fabricating accurate short-span, screw-retained implant supported fixed dental prostheses.

## Bibliography

---

- <sup>i</sup> Branemark, P.I. (1983) Osseointegration and its experimental background. *Journal of Prosthetic Dentistry*.50: 399–410.
- <sup>ii</sup> Jemt T, Lekholm U, Adell R. Osseointegrated implants in the treatment of partially edentulous patients: A preliminary study on 876 consecutively placed fixtures. *Int J Oral Maxillofac Impl* 1989; 4 (2): 211-17.
- <sup>iii</sup> Lekholm U, van Steenburghe D, Herrmann I, Bolender C, Folmer T, Gunne J, Henry P, Higuchi K, Laney WR, Linden U. Osseointegrated implants in the treatment of partially edentulous jaws: A prospective 5-year multicenter study. *Int J Oral Maxillofac Impl* 1994; 9 (6): 627-35.
- <sup>iv</sup> Attard NJ, Zarb GA. Implant prosthodontic management of partially edentulous patients missing posterior teeth: The Toronto experience. *J Prosthet Dent* 2003; 89 (4): 352-9.
- <sup>v</sup> Wood MR, Vermilyea SG. A review of selected dental literature on evidence-based treatment planning for dental implants. Report of the committee on research in fixed prosthodontics of the Academy of Fixed Prosthodontics. *J Prosthet Dent* 2004; 92 (5): 447-62.
- <sup>vi</sup> Philip C, Edmond H, Ching S, Edward C, Chow T. Dental Implant Practice Among Hong Kong General Dental Practitioners in 2004 and 2008. *Implant Dentistry*. 2011; 20(1): 95-105
- <sup>vii</sup> Turbush SK., Turkyilmaz I. Accuracy of three different types of stereolithographic surgical guide in implant placement: An in vitro study. *The Journal of prosthetic dentistry*. 2012. 108(3), 181-188.
- <sup>viii</sup> Image Courtesy Dr. Edwin McGlumphy
- <sup>ix</sup> Craig's Restorative Dental Materials. 12th ed. 2006, Mosby. 270-332
- <sup>x</sup> Duke, P., et al., Study of the physical properties of type IV gypsum, resin containing, and epoxy die materials. *J Prosthet Dent*, 2000. 83(4): p. 466-73.

- 
- <sup>xi</sup> Walker, M.P., D. Ries, and B. Borello, Implant cast accuracy as a function of impression techniques and impression material viscosity. *Int J Oral Maxillofac Implants*, 2008. 23(4): p. 669-74.
- <sup>xii</sup> Assif, D., B. Marshak, and A. Schmidt, Accuracy of implant impression techniques. *Int J Oral Maxillofac Implants*, 1996. 11(2): p. 216-22.
- <sup>xiii</sup> Wostmann, B., P. Rehmann, and M. Balkenhol, Influence of impression technique and material on the accuracy of multiple implant impressions. *Int J Prosthodont*, 2008. 21(4): p. 299-301.
- <sup>xiv</sup> Ceyhan, J.A., G.H. Johnson, and X. Lepe, The effect of tray selection, viscosity of impression material, and sequence of pour on the accuracy of dies made from dual-arch impressions. *J Prosthet Dent*, 2003. 90(2): p. 143-9.
- <sup>xv</sup> Assuncao, W.G., H.G. Filho, and O. Zaniquelli, Evaluation of transfer impressions for osseointegrated implants at various angulations. *Implant Dent*, 2004. 13(4): p. 358-66.
- <sup>xvi</sup> Howell K, McGlumphy E. Accuracy of the Biomet 3i Encode® Robocast™ technology versus conventional implant impression. Masters of Science Thesis. Columbus, Ohio : Ohio State University, 2011
- <sup>xvii</sup> Howell KJ, McGlumphy EA, Drago C, Knapik G. Accuracy of the analog placement by the Encode® Robocast™ technology against traditional methods of open (pick-up) and closed (transfer) tray impressions. *Int J Oral Maxillofac Implants*. 2013 Jan-Feb;28(1):228-40.
- <sup>xviii</sup> Eliasson A, Ortorp A. The Accuracy of an implant impression technique using digitally coded healing abutments. *Clinical Imp Den and Related Research*. May 2012 ;Vol14 Suppl 1:e30-8.
- <sup>xix</sup> Khaled Al-Abdullah, Roya Zandparsa, Matthew Finkelman, Hiroshi Hirayama, An in vitro comparison of the accuracy of implant impressions with coded healing abutments and different implant angulations. *J Prosth Dent*, Vol110, Issue 2, Aug 2013, Pg90-100,
- <sup>xx</sup> Mormann, W.H., et al., Chairside computer-aided direct ceramic inlays. *Quintessence Int*, 1989. 20(5): p. 329-39.
- <sup>xxi</sup> Duret, F., J.L. Blouin, and B. Duret, CAD-CAM in dentistry. *J Am Dent Assoc*, 1988. 117(6): p. 715-20.

- 
- xxii Mormann, W.H., The evolution of the CEREC system. *J Am Dent Assoc*, 2006. 137. Suppl: p. 7S-13S.
- xxiii Logozzo S, Zanneti E, G Franceschini, Kilpela A, Makynen A. Recent advances in dental optics – Part I: 3D intraoral scanners for restorative dentistry. *Optics and Lasers in Engineering*. 54(2014)203–221
- xxiv Vander Meer WJ, Andriessen FS, Wismeijer D, Ren Y. Application of Intra-Oral Dental Scanners in the Digital Workflow of Implantology *PLoS One*. 2012
- xxv Hyun-Soon Pak, Han JS, Lee JB, Sung-Hun Kim, and Yang J. Influence of porcelain veneering on the marginal fit of Digident and Lava CAD/CAM zirconia ceramic crowns. *J Adv Prosthodont*. 2010 June; 2(2): 33–38.
- xxvi Andreas Syrek, Gunnar Reich, Dieter Ranftl, Christoph Klein, Barbara Cerny, Jutta Brodesser, Clinical evaluation of all-ceramic crowns fabricated from intraoral digital impressions based on the principle of active wavefront sampling, *Journal of Dentistry*, Volume 38, Issue 7, July 2010, Pages 553-559.
- xxvii Nayyar N, Yilmaz B, McGlumphy E. Using digitally coded healing abutments and an intraoral scanner to fabricate implant-supported, cement-retained restorations. *J Prosthet Dent* 2013;109:210-215.
- xxviii Wei-Shao Lin, Bryan T. Harris, Zandinejad A, Dean Morton. Use of digital data acquisition and CAD/CAM technology for the fabrication of a fixed complete dental prosthesis on dental implants. *Journal of Prosthetic Dentistry* - January 2014. Vol. 111, Issue 1, Pages 1-5.
- xxix T. Jemt. Failures and complications in 391 consecutively inserted fixed prostheses supported by Brånemark implant in the edentulous jaw: a study of treatment from the time of prostheses placement to the first annual checkup. *Int J Oral Maxillofac Implants*, 6 (1991), pp. 270–276
- xxx Kan JK, Rungcharassaeng K, Bohsali K, Goodacre CJ, Lang BR. Clinical methods for evaluating implant framework fit, *The Journal of Prosthetic Dentistry*, Volume 81, Issue 1, January 1999, Pages 7-13
- xxxi White GE. Herstellung eines Gerüsts für eine implantatgetragene Totalprothese im Unterkiefer. In: White GE (ed). *Implantat-Zahntechnik*. Berlin: Quintessenz, 1993:S 114.

- 
- <sup>xxxii</sup> Tan PL1, Gratton DG, Diaz-Arnold AM, Holmes DC.' An in vitro comparison of vertical marginal gaps of CAD/CAM titanium and conventional cast restorations.' J Prosthodont. 2008 Jul;17(5):378-83
- <sup>xxxiii</sup> Drago C, Saldarriaga RL, Domagala D, Almasri R. 'Volumetric determination of the amount of misfit in CAD/CAM and cast implant frameworks: a multicenter laboratory study'. Int J Oral Maxillofac Implants. 2010 Sep-Oct;25(5):920-9.
- <sup>xxxiv</sup> Lee, K.B., et al. Marginal and internal fit of all-ceramic crowns fabricated with two different CAD/CAM systems. Dent Mater J, 2008. 27(3): p. 422-6.
- <sup>xxxv</sup> <http://www.datron.com/dental-milling.php>
- <sup>xxxvi</sup> Geomagic DesignX 2014 User Guide. Page 883-889
- <sup>xxxvii</sup> Clelland, N. L., Papazoglou, E., Carr, A. B. and Gilat, A. (1995), Comparison of Strains Transferred to a Bone Simulant Among Implant Overdenture Bars with Various Levels of Misfit. Journal of Prosthodontics, 4: 243–250.